AD NUMBER

AD915257

LIMITATION CHANGES

TO:

Approved for public release; distribution is unlimited.

FROM:

Distribution authorized to U.S. Gov't. agencies only; Test and Evaluation; 15 DEC 1973. Other requests shall be referred to Army Missile Command, Attn: AMSMI, Redstone Arsenal, AL 35809.

AUTHORITY

DARPA ltr, 17 Jun 1974

DREV R-690/73
PROJ. 95-51-10

NON CLASSIFIÉ
UNCLASSIFIED

ABSOLUTE ELECTRON DENSITY MEASUREMENTS IN TURBULENT HYPERSONIC SPHERE WAKES WITH LANGMUIR PROBES

D. Heckman, L. Sevigny and A. Emond

CENTRE DE RECHERCHES POUR LA DÉFENSE
DEFENCE RESEARCH ESTABLISHMENT
VALCARTIER

DEFENCE RESEARCH BOARD
CONSEIL DE RECHERCHES POUR LA DÉFENSE

Québec, Canada

October/octobre 1973


ACCESSION for
NTIS White Section
DDC Buff Section
UNANNOUNCED
JUSTIFICATION
BY
DISTRIBUTION/AVAILABILITY CODES
Dist. AVAIL. and/or SPECIAL
B

(14)
DREV-R-690/73
~~PROJ. 95-51-10~~

NON CLASSIFIE
UNCLASSIFIED

(6) ABSOLUTE ELECTRON DENSITY MEASUREMENTS IN TURBULENT HYPERSONIC SPHERE WAKES WITH LANGMUIR PROBES,

by

(10) D./Heckman, L./Sévigny [redacted] A./Emond

(11) Oct 73

(12) 60 p.

This research was sponsored jointly by

The Defence Research Establishment
Valcartier
P.O. Box 880
Courcelette, Québec, Canada
Under Project D-95-51-10

The Advanced Research Projects Agency
(ARPA) Order-133
Monitored by the U.S. Army Missile Command,
Redstone Arsenal, Alabama 35809
Contract ~~DA-H01~~-69-C-0921

(15)

CENTRE DE RECHERCHES POUR LA DEFENSE
DEFENCE RESEARCH ESTABLISHMENT
VALCARTIER
Tel: (418) 844-4271

Québec, Canada

404915

October/octobre 1973

RESUME

On a mesuré, dans un des tunnels balistiques du Centre de recherches pour la défense, Valcartier (CRDV), la valeur absolue de la densité des électrons se trouvant dans le sillage ionisé produit par une sphère hypersonique de 2.7 pouces de diamètre, projetée à une vitesse de 14,500 pieds/seconde, dans de l'air à 10 torr. La technique expérimentale utilise des sondes de Langmuir dont les possibilités théoriques pour une telle expérience ont été démontrées par G.W. Sutton. Un soin tout particulier a été apporté à la réalisation de certains détails de l'expérience, telles la propreté des sondes. la minimisation des perturbations de l'écoulement et la réduction de l'intensité des ondes de choc réfléchies. La valeur de la densité électronique déduite des données fournies par les sondes de Langmuir est en accord avec celle obtenue par des mesures simultanées à l'aide d'un interféromètre micro-onde. On a également déterminé le comportement du potentiel de plasma dans le sillage. Celui-ci semble avoir tendance à se maintenir près du potentiel de la sonde la plus fortement polarisée, mais on n'a pu établir la raison de ce comportement. En conclusion, on suggère d'autres applications possibles de l'appareillage expérimental. (N C)

ABSTRACT

Measurements were carried out in the ballistic range facilities at DREV of the absolute electron density levels in the wakes of 2.7 inch diameter spheres flown at 14,500 feet/second in air atmospheres at 10 torr. The experimental technique involved the use of Langmuir probes, following the theoretical demonstration of feasibility of such an experiment by G.W. Sutton. Considerable attention was paid to details of the experiment, such as probe cleanliness, minimum flow disturbance and the minimization of reflected shocks. Electron density level estimates obtained with the Langmuir probes were in good agreement with electron density estimates derived from simultaneous measurements with a microwave interferometer. The behavior of the plasma potential in the wake was also determined; the plasma potential apparently attempted to maintain itself close to the potential of the most highly biased probes, but the reason for this behavior has not been established. This Report concludes with suggestions for further utilization of the equipment. (U)

TABLE OF CONTENTS

1.0 INTRODUCTION

The determination of the behavior of the electron density in the turbulent ionized wakes behind hypersonic projectiles has been of considerable interest for at least a decade. Measurements of the spatially averaged electron density in the wakes of spheres and cones have been in existence for some time (1 - 3)*; current interest is oriented towards spatially resolved measurements of the average and fluctuation levels of electron density (4 - 9). On the one hand, electron density data is useful for testing theoretical models of the physical processes in turbulent wakes (10 - 15) but, on the other, knowledge of the behavior of the electron density in the wake is essential to the modeling of the scattering of incident microwave radiation by wakes (16 - 18).

Up to the present, the only reliable data concerning the average electron density in a wake were those obtained with microwave interferometer and cavity techniques (1 - 3). Attempts have also been made recently to deduce ion density levels in sphere wakes through the use of arrays of spherical and cylindrical electrostatic ion probes distributed across the wake. Sévigny et al. (19) employed a number of static and kinetic continuum probe theoreis for the interpretation of the current collected by their cylindrical ion probes in 2.7 inch diameter sphere wakes, together with the experimentally determined temperature and velocity distributions. The agreement between the ion densities deduced by them from kinetic theory and the values of the electron density obtained with a two-channel microwave interferometer was within a factor of about two at axial distances of a few hundred diameters and a pressure of 7.6 torr. However, in the near wake, and at higher pressures, the indicated discrepancy was of the order of a factor of ten. French et al. (20 - 21) employed a somewhat different approach: instead of applying the available theories, they attempted to develop a correlation between ion density and probe current for spherical probes in a shock tube, subsequently applying this correlation to

measurements made in a wake. They evaluated their results by computing an ion density line integral $\overline{n_i D_p}$ across the wake, and then comparing with equivalent estimates of $\overline{n_e D_p}$ from microwave measurements. The agreement achieved was within a factor of 2 - 3, extending over a range of axial distance from 600 to 10,000 diameters. (Here n_i represents the positive ion density, n_e the electron density, and D_p is an effective diameter for the ionized portion of the wake). Of course since the various probe theories and correlations express a relationship for the probe current which may depend on temperature, density, and velocity as well as ion density, the interpretation of probe current in terms of ion density fluctuations is fraught with difficulty (19).

Recently G.W. Sutton (1969) has examined the feasibility of performing measurements with fine-wire Langmuir probes of the properties of the electron density in the turbulent wakes of projectiles flown in ballistic ranges. A true Langmuir probe must be used at low density so that the electron-neutral particle mean-free path λ_{e-n} is much larger than a convenient probe diameter. However, if one wishes to study turbulent wakes, the Reynolds number (depending directly on density) must be large enough for the wake to be turbulent. Both of these conditions can be satisfied if one can fly large diameter projectiles at low pressures. Turbulent wakes are generally observed when $P_\infty D$ exceeds 15 torr inches, where P_∞ is the ambient range pressure and D is the projectile diameter. At a range pressure of 10 torr, D must exceed 1.5 inches. This compares favorably with the 2.7 inch diameter spheres which are routinely launched at 15,000 feet/second on the DREV Range 5 facility. Sutton was the first to point out that if these typical test conditions were employed in a ballistic range to study turbulent wakes, fine cylindrical probes could be operated using wire diameters much smaller than an electron mean-free path. Thus collisionless cylindrical probe theory could be applied. For cylindrical Langmuir probes operating at electron saturation, the collisionless theory indicates that the current drawn by the probes is sensitive only to the electron density (22). It can therefore be assumed that the fluctuations observed in the current to a cylindrical probe are dominated by the fluctuations in the electron density, and can be used to deduce the statistics of these fluctuations.

It follows that the application of Langmuir probes to the measurement of electron density behavior in a hypersonic turbulent wake is of very great potential interest. This report is concerned with measurements of the average levels of electron density in the turbulent wakes of 2.7 inch diameter spheres fired at 14,500 feet/second in dry air atmospheres.

2.0 LANGMUIR PROBE THEORY

According to Langmuir and Mott-Smith (7, 23), the current density to a cylindrical free-molecular probe is given by

$$j_e = \frac{n_e\, e\, c_e}{4} \left\{ \frac{r_s}{r_p} \left[\operatorname{erf} \left(\frac{r_p^2}{r_s^2 - r_p^2}\, \phi^* \right)^{\frac{1}{2}} \right] + \exp(\phi^*) \operatorname{erfc} \left(\frac{r_s^2}{r_s^2 - r_p^2}\, \phi^* \right)^{\frac{1}{2}} \right\} \tag{1}$$

Here $c_e = \left(\frac{8k\, T_e}{\pi\, m_e} \right)^{\frac{1}{2}}$ where T_e is the electron temperature

k is the Boltzman constant

and m_e is the electron mass

n_e is the electron density

r_s is the sheath radius

r_p is the probe radius

ϕ^* is the normalized probe potential eV/kT

Under conditions of operation where the probe is strongly biased ($\phi^* >> 1$) and the sheath radius to probe radius is large ($(r_p^2/r_s^2)\phi^* << 1$), Equation 1 becomes

$$j_e = \frac{n_e\, e\, c_e}{4} \quad \frac{2}{\sqrt{\pi}}\ (1 + \phi^*)^{\frac{1}{2}}$$

or

$$j_e = \frac{n_e\, e^{3/2}\, 2^{\frac{1}{2}}\, V^{\frac{1}{2}}}{\pi\ m_e^{\frac{1}{2}}} \tag{2}$$

For $r_s/r_p \to \infty$ and values of $\phi^* > 10$, Equation 2 can be used instead of Equation 1 to an accuracy of 5%.

Recently, collisionless probe theory has been studied by Laframboise (24). For a ratio of Debye length to probe radius $\lambda_{De}/r_p >> 1$, his results correspond exactly to Equation 1 (7), and they also indicate that Equation 2 is still quite accurate for values of λ_{De}/r_p as small as 0.4. For example, given $\phi^* \geq 10$ and $r_s^2/r_p^2 >> 1$, the error in Equation 2 is about 12% for $\lambda_{De}/r_p = 1$ and about 2% for $\lambda_{De}/r_p = 2$.

The approximate range of values of the various theoretical parameters governing probe operation were estimated from the results of flow field calculations. Approximate computations were made of the flow at 15,500 feet/second in a 10 torr air atmosphere. First, calculations of the inviscid flow field were used to establish the conditions along a surface representing the average position of the front between the turbulent core and the inviscid part of the wake. In the computational model any fluid transported across the front into the core was assumed to be instantaneously and completely microscopically mixed with all the chemical species contained within the front. The resulting predictions for the flow variables varied with axial distance but were constant across the wake. From these approximate estimates of temperature, velocity, electron density, mass density and species concentrations, the behavior of the various probe parameters was calculated (7, 15). Figure 1 (which is taken from G.W. Sutton's paper (7)) shows the calculated average electron mean free path and the predicted behavior of the Debye length.

To compute the Debye length, Sutton assumes the electron temperature is equal to the gas temperature (7). The vibration equilibration time for nitrogen is extremely rapid, so that as cold nitrogen is ingested by the turbulent wake, the average vibrational temperature should decrease at the same rate as the translational temperature. The electron temperature, which is probably in equilibrium with the nitrogen vibrational temperature, should follow the translational temperature.

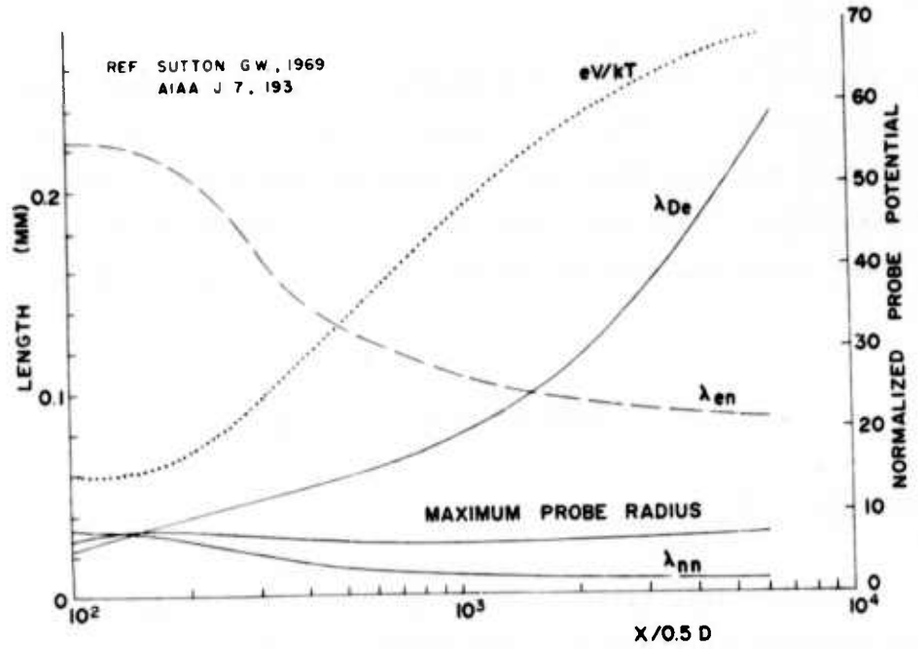

FIGURE 1 - Variation of probe parameters with axial distance in the wake of a 2.7 inch diameter sphere flown at 15,500 feet/second in air at 10 torr predicted by theoretical calculations at AVCO. The probe bias was assumed to be 2 volts with respect to the plasma potential.

Figure 1 also shows the maximum allowable probe radius if contributions to the probe current effected by means of collisions made by the incident electrons in the sheath are to be held to less than 20% of the orbital limited probe current defined by Equation 2. For axial distances exceeding 100 body diameters (B.D.), Figure 1 indicates that both λ_{De}/r_p and λ_{e-n}/r_p exceed unity. However, the relative magnitudes of λ_{e-n} and λ_{De} are such that multiple collisions can occur in the probe sheath at axial distances approaching 1000 diameters. For conditions appropriate to those at DREV, Sutton deduced that a probe of radius equal to 0.001 inch or less will ensure that the effect of collisions on the probe current will be less than 20%. (For details of this analysis, the original paper should be consulted (7)).

Consideration must also be given to the neutral-neutral mean-free path. A small neutral-neutral mean-free path coupled with a cold probe can depress the temperature of the gas in the vicinity of the probe. This causes in turn a higher density in the vicinity of the probes,

thereby reducing the electron mean-free path. Figure 1 shows that the neutral-neutral mean-free path is small compared to the electron-neutral mean-free path and less than half the maximum probe radius for the collisional effect to be less than 20%. To be conservative, Sutton suggests the probe diameter should be made as small as possible.

3.0 EXPERIMENTAL TECHNIQUE

3.1 Langmuir Probes

The Langmuir probe investigation of electron density in air wakes was the last of the major wake experiments to be undertaken at DREV, and did not become operational until 1970. The objectives of this experiment were to measure the average level of electron density in the wake and the statistics of the fluctuations. The configuration of Langmuir probes chosen for these tasks was very similar to the array of electrostatic probes previously used at DREV (25). The use of an array allows observations of both scale data and space-time correlations to be obtained in addition to the mean density measurement.

Because of the time factor, an attempt was made to go in one step from the initial concept of the experiment to the final full-scale realization. Considerable attention was devoted to details of the experimental setup. While the large diameter projectile capability at DREV permits the use of larger diameter probes, it also leads to the need for a larger supporting structure. The main design objectives of importance to the measurement included maximum structural rigidity (to protect the probes), minimum interference with the wake flow, minimum generation of reflected shock waves from the supporting structure, and finally, facility for ensuring probe cleanliness.

Figure 2 shows the supporting structure. Two semiannular perforated plates are held together with thin wedgelike spacers to form a rigid rectangular structure (or mainframe); the plates and the wedges

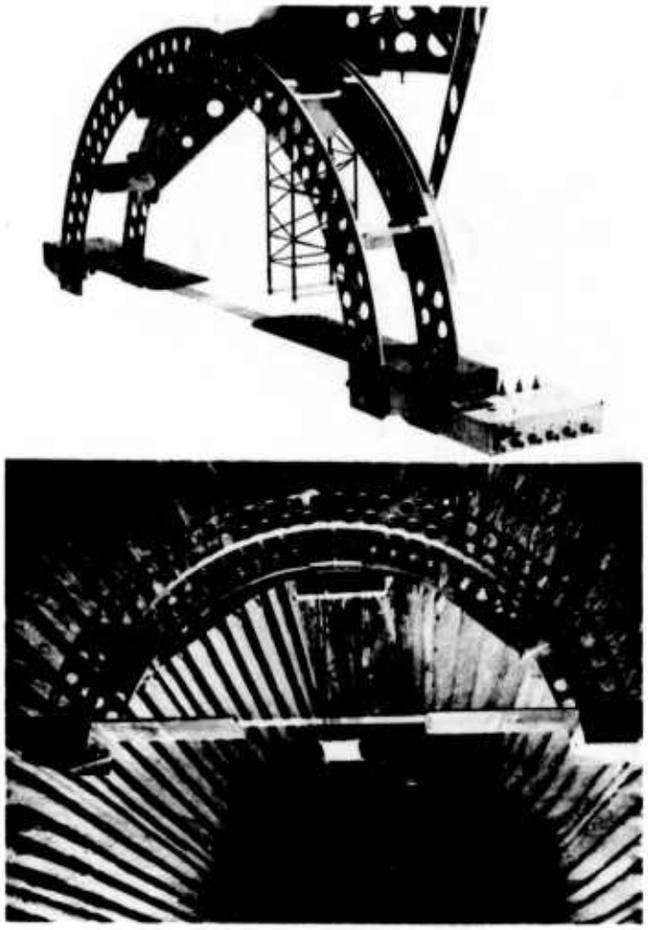

FIGURE 2 - Support for the Langmuir probes, photographed in the studio (top) and installed in the range (bottom). The preamplifiers are mounted in the box at the right (top). The range is lined with fiberglas wedges (bottom).

are aligned with the radius vector originating normally from the axis of flight of the range and are sharp-edged to minimize shock reflections. In fact most of the outgoing shock wave systems from a hypersonic projectile will simply pass through the structure to be dissipated in the fiberglas wedge treatment with which the range is lined (26). The inside semiannular radius is 20 inches; the spacing between the plates is 6 inches. NACA 0012 aerofoil-shaped probe-supports project from near each end of the semiannular mainframe in a horizontal plane nominally 3 inches above the line of flight; consequently the angle between the normal to the outgoing shock front and the aerofoil is very small and little reflection can occur. The sixteen inch gap between the ends of the aerofoils is

bridged with a network of cantilevered telescoped hollow Degussit aluminium oxide ceramic tubing, held at one end in channels cut along the interior of the supporting aerofoils, and interbraced with small pieces of ceramic rod, soldered in place with glass (Figure 3). The largest ceramic tube adjacent to the aerofoil is 2 millimeters in diameter, followed by a 1.2 millimeter diameter section, and finally, at the center by a 3 centimeter length of 0.5 millimeter diameter. In the present research there were four probes with an interprobe spacing of 0.5 inch.

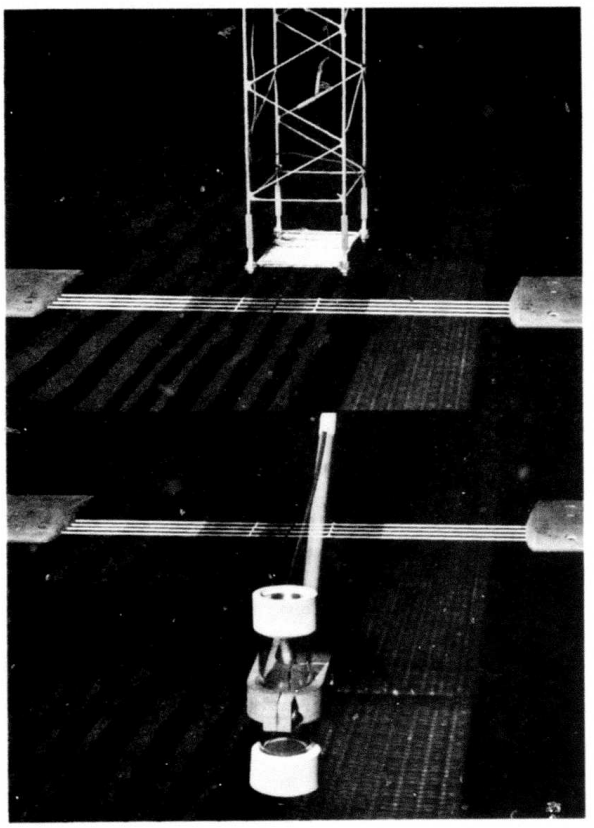

FIGURE 3 - Closeups of the Langmuir probes with the reference grid in place (top) and with the plasma scrubber in place (bottom).

Thus the final supporting structure adjacent to the active probe element is very small and of the order of the size investigated by Ghosh and Richard (27) in their study of interference effects on a downstream probe by an upstream probe. The annealed platinum alloy wire is threaded through the hollow ceramic tube and a short 2 millimeter or 4 millimeter length of fine wire is exposed to the range atmosphere in the centre midway between the aerofoils. Junction boxes are located close to the aerofoil tips, allowing the wires to be soldered in place. Channels for up to seven probes run the length of the molded aerofoil and solid coaxial connectors are used from the junction box to the preamplifiers located at the other end. The preamplifiers, essentially current-to-voltage operational amplifiers, also supply the probe bias voltages. The feedback resistor in the preamplifier is usually 200 kilohms and the frequency response as measured with the collecting probe wires and coaxial connectors in place is flat within 1 dB from 0 to 300 kiloHertz. The return grid (Figure 3) consists of about 240 turns of 0.001 inch diameter wire on a 6 inch by 4 inch rectangular grid, supported on isolating posts on an open frame for minimum shock and flow disturbance. The collecting wires and the return grid were fabricated with annealed Sigmund Cohn #851 platinum alloy (Pt-0.79/Rh-0.15/Ru-0.06) wires; both 0.001 inch and 0.0005 inch diameter wire were used. The actual wire diameters were checked by photographing them with a calibrated scale using a 300X and 600X optical microscope.

Considerable thought was given to probe surface cleanliness. The irreproducibility possible with unclean probes has been observed in many laboratories and was documented by Whener and Medicus (28). In steady-state plasmas the usual technique is to subject the probe to red-to-white heat using electron or ion bombardment induced by biasing the probe positively or negatively with respect to the steady plasma. This procedure is not directly possible in the wake because the hypersonic wake in a ballistic range is a transient plasma lasting only a few tens of milliseconds. Two solutions were considered: heating the probe by passing an electric current along the wire or actually designing

into the Langmuir probe system a separate plasma source for bombardment heating. Both techniques are feasible; the second was adopted because it is the standard method for steady plasmas and thus offers the greater credibility for the experiment.

The plasma source employed is a modified brush cathode of the type reported by K.-B. Perrson (29). A plane graphite cathode is inserted in one side of a six inch long two inch diameter pyrex tube, while a stainless steel annular anode is flush mounted on the other end, and held in place by a molded ceramic cap (Figure 4). This type of discharge produces a negative glow which starts near the cathode and extends through and beyond the annular anode. Experience at DREV, mainly with inverse brush cathodes (30) variously fabricated of aluminum, stainless, and graphite, has led to the use of plane graphite as a cathode. Metallic cathodes sputter and cathode material tends to deposit over the walls of the discharge tube, eventually spoiling the discharge.

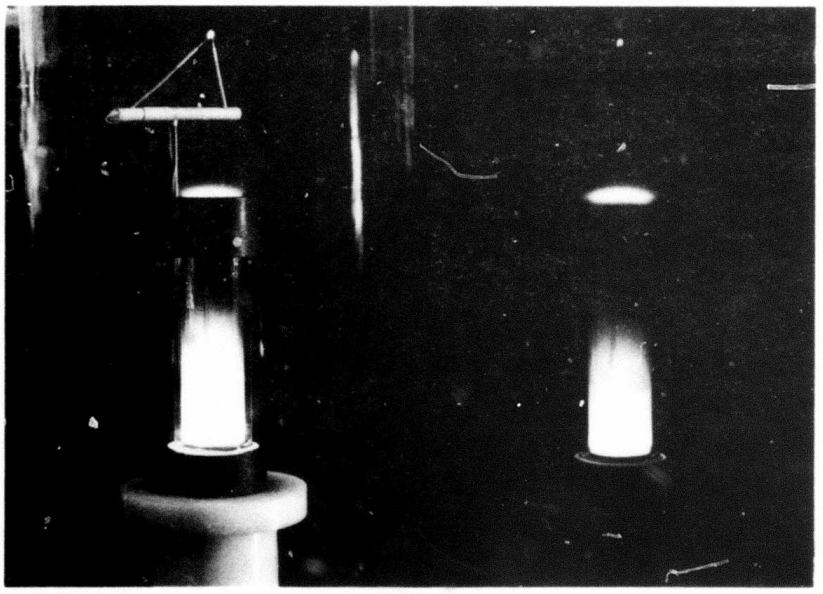

FIGURE 4 - Illustration of the plasma scrubber in action. A make-shift probe is shown at the right.

Probe cleaning is carried out late in the firing sequence. The mainframe is installed in the range on the day previous to a firing, with loops of wire in place. Once all electrical connections are made, the wires are drawn taut and soldered in place at the aerofoil tip junction boxes. The probes are photographed in place, using a scale, to establish probe length and interprobe spacing. The range is then cleared and evacuated to about 70 microns - a three to four hour process. When all the procedures of loading the gun etc. have been completed, probe scrubbing is initiated. To clean the probes, the discharge tube is first rotated into place so that the discharge is aligned with the probes (Figure 3). At the same time, the return grid is rotated out of the vicinity of the probes. Cleaning is carried out in an atmosphere of mainly dry nitrogen at a pressure of about 0.3 torr. Discharge stability is checked and then the discharge potential is increased to between 900 and 1000 volts. The probes are grounded through individual potentiometers which are used to equalize the current drawn to each probe. The electron currents drawn to the probe wires are slowly and carefully increased by raising the discharge potential until the wires are glowing either dark yellow or bright yellow, depending on wire diameter. The wires are held at temperature for about 2 minutes, then the discharge is extinguished, the discharge tube rotated out of the way, the return grid (Figure 3) rotated into place, and the range brought up to firing pressure (usually 10 torr) with dry air. It takes about 10 minutes from the end of cleaning to achievement of firing pressure, the time being determined essentially by the volume of the range (10 feet in diameter by 425 feet in length). However, an additional short delay has normally been countenanced to permit a final phase adjustment to the two channels of an X-band focussed beam sine-cosine interferometer system. After the firing, a gate valve is closed to prevent air re-entering the range tank from the dump tank to minimize probe damage, and a slow re-entry of air is made to bring the range pressure up to atmospheric. It has been observed that during the heating associated with cleaning, some changes may occur in the amount of wire exposed, so wire lengths are measured from photographs taken after the firing. With this cleaning technique the results have been found reasonably reproducible. In view of published

reports (31) on the rapid decay of probe 'cleanliness' with elapse of time after bombardment cleaning, a few rounds were expended with the time between cleaning and firing reduced to between 5 and 10 minutes, but no obvious differences in results were observed. (On a smaller range, the time delay could be much reduced).

As was intended, the Langmuir probe equipment has been operated in two modes. In Mode 1 (or the absolute electron density measurement mode), the 5 active probes are operated with different bias voltages, to permit the simultaneous determination of the behavior of the plasma potential V_p and the electron density n_e. From Equation 2

$$(j_e)_i \sim n_e (V_i - V_p)^{\frac{1}{2}} \qquad (3)$$

where i designates any one of the four probes, and where the effective probe potential has been written explicitly as the difference between the applied bias voltage V_i and the plasma potential V_p, the currents measured in Mode 1 with any pair of probes operated at different bias can be used to solve for n_e and V_p.

In Mode 2, the 4 active probes are operated with the same strong bias so that V_p is negligible compared to V_i. In this case $(j_e)_i \sim n_e V_i$ and fluctuations in the probe current density $(j_e)_i$ should be solely due to fluctuations in n_e. This mode not only gives an estimate of the average electron density but should also provide the required data on electron density fluctuation scales, etc.

Both modes of operation were used in these studies. Some surprises were encountered and these will be described later.

The signals from the probes were recorded in pairs on 35 millimeter film using Fastax cameras and Tektronix 550 and 555 oscilloscopes. The probe preamplifiers were used to drive the eight to ten feet of cable required to lead the signals to the exterior of the range flight chamber.

In order to facilitate the oscilloscopic DC recording of the transient probe signals at high gains, the bias voltages were subtracted from the output of the preamplifiers through the use of Type 'O' operational amplifiers. The net signals were passed through broadband (0 - 1 MHz) type HP 467A power amplifiers and transmitted over long terminated 92 ohm cables to the Range 5 recording room, where they were recorded in various combinations. A more detailed description of the characteristics of the recording system has been published (8).

3.2 Microwave Interferometer

In a microwave interferometer, a common microwave source is used to feed two distinct microwave channels or arms, a 'reference' arm and a 'transmission' arm, in such a way that the phase difference between the signal at the output of the transmission arm and the signal at the output of the reference arm can be compared. In the absence of any difference in the dielectric media in the two arms, this difference in phase depends only on the difference in the number of wavelengths between the two arms. Now, if a medium of different dielectric constant is inserted somewhere in the transmission arm, an additional shift in the phase difference between the two arms will be detected. Normally, in the operation of an interferometer, the difference in phase due to path length difference between the two arms is adjusted to some desired value before a measurement. During the measurement, the additional phase shift resulting from the introduction of some peturbation in the transmission arm is detected and recorded as a function of time. When the perturbation is due to an ionized plasma, it is possible to utilize the observed phase shift to infer the charge density levels in the plasma, provided these fall within certain limits.

Figure 5 is a schematic representation of the two-channel interferometer system installed on Range 5. The microwave transmitter source is operated in the X_s-band at 9.60 GHz (λ = 3.1227 cm). The choice of frequency was dictated by the desire to have sensitivity to

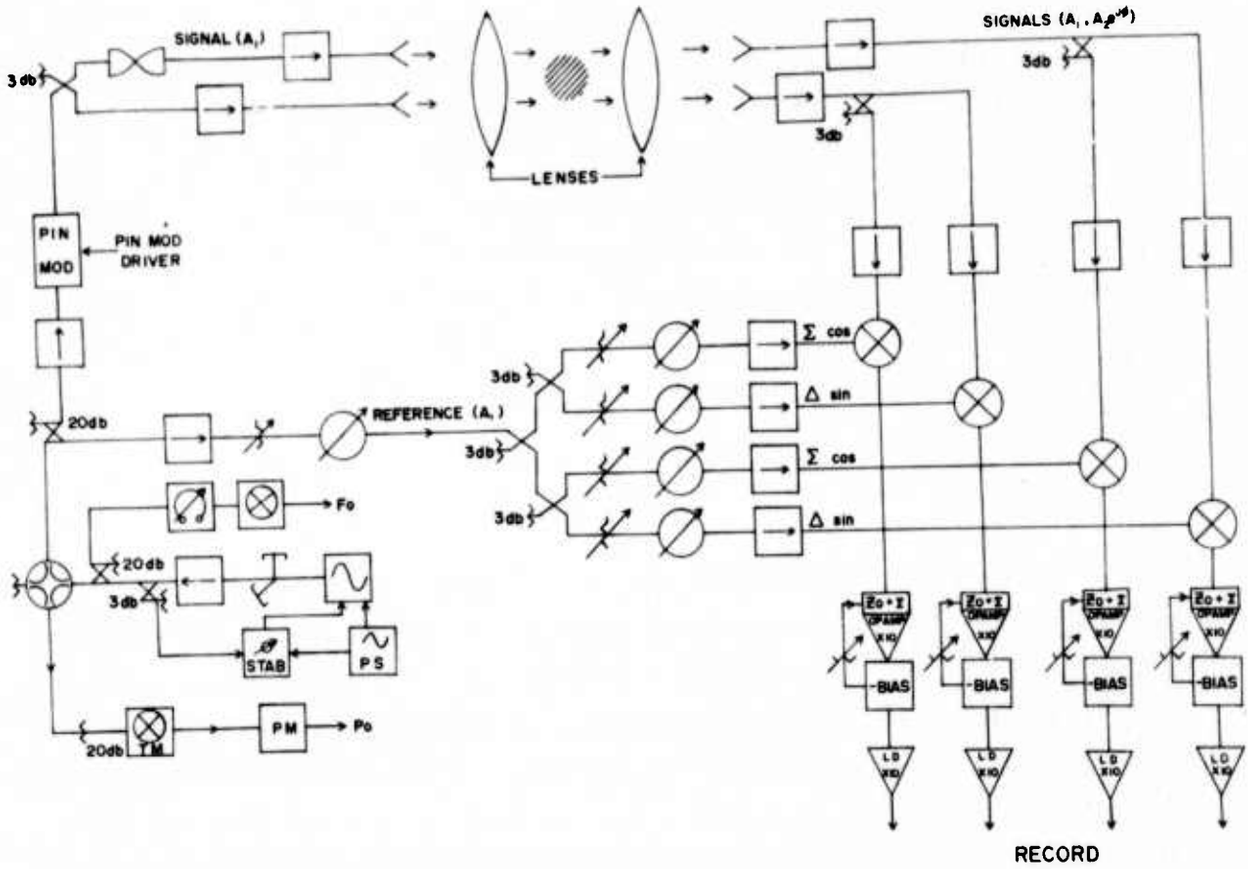

FIGURE 5 - Schematic of DREV two channel X_s-band interferometer.

electron densities in the range from 10^{11} to 10^9 electrons/cc while retaining as much resolution as possible. The transmitter source is a Varian V-58 0.5 watt reflex klystron, with phase-lock frequency stabilization provided by a Microwave Specialities MOS-1 Stabilizer operating through the reflector circuit and the Hewlett Packard Model 416 B power supply unit. A high-directivity (-40 dB) top-wall coupler is used to separate the transmission path from the reference path; the two arms are then directed in separate ways. The reference arm is led underneath the range tank. The transmission arm is divided into two channels; these are oriented to illuminate, via conical antennae, two regions in the center of the range approximately 3/4 inch above and below the centerline. A Hewlett Packard 8735 A PIN modulator with large dynamic range is inserted into the transmission arm before its division into two channels; the transmitted signal is normally gated off with this modulator for short periods during a recording to provide a continuous absolute determination of the DC baseline level (32).

The projectile is launched along the range centerline and the ionized wake behind the projectile fills the region illuminated by the transmitter horns and scanned by the receiver horns. A double lens focussing system (Figure 6) is interposed between the transmitting and receiving antennae to increase the resolution of the system. With this lens system a beam width of approximately 2 inches or 0.74 of the diameter of a 2.7 inch diameter sphere is obtained, based on the -3 dB contours of the channel beam (Figure 7). The depth of field over which the beam remains at constant width (to within ± 10%) is about 12 inches or about 5 diameters (33). Based on the schlieren wake width, this appears to be adequate for measurements of 2.7 inch diameter sphere wakes to at least 400 diameters behind the projectile.

The microwave energy beams transmitted across the lens systems are directed through the receiver antennae to the entry ports of various hybrid mixers. A sample of reference signal power is directed to the other entry port of each mixer. The reference signal power level is roughly 100 times the transmitted arm signal level. The mixed reference and transmitted signals are impressed on MA-611 low noise crystal detectors incorporating IN-23G crystals. The crystals are driven into the middle of their linear response regions by the large reference signal levels and are operated into low noise 10 kilohm video loads. These video loads comprise part of the input networks of Tektronix Type 'O' operational amplifier plug-ins which permit subtraction of the large DC component due to the reference signal, before a further amplification of 100 times.

The signals are recorded on polaroid film via Tektronix Type 550 and 555 oscilloscopes and represent nominally $SIN(\Delta\phi(t))$ or $COS(\Delta\phi(t))$ where $\Delta\phi(t)$ is the phase shift induced by the presence of the ionized wake in the transmission arm. Sweep speeds and sensitivities are supplied in various conbinations to permit an optimum recording of the signals.

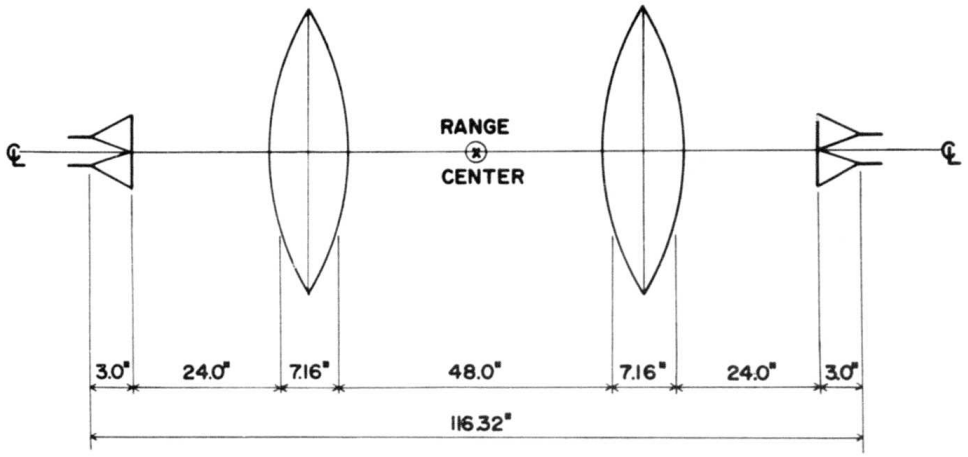

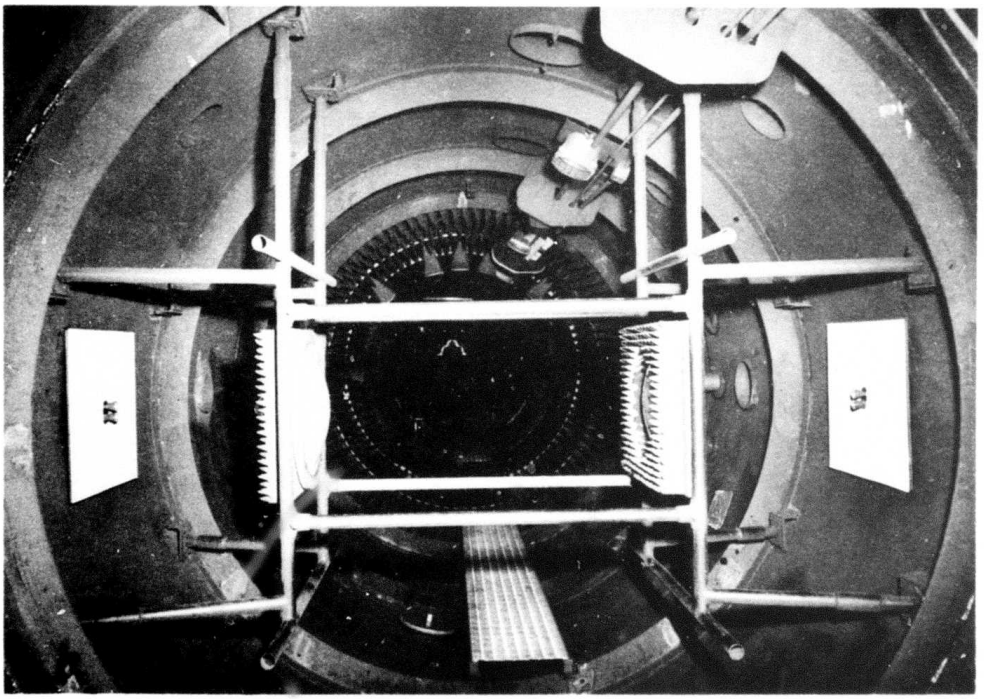

FIGURE 6 - Interferometer station layout in schematic (top) and as photographed (bottom).

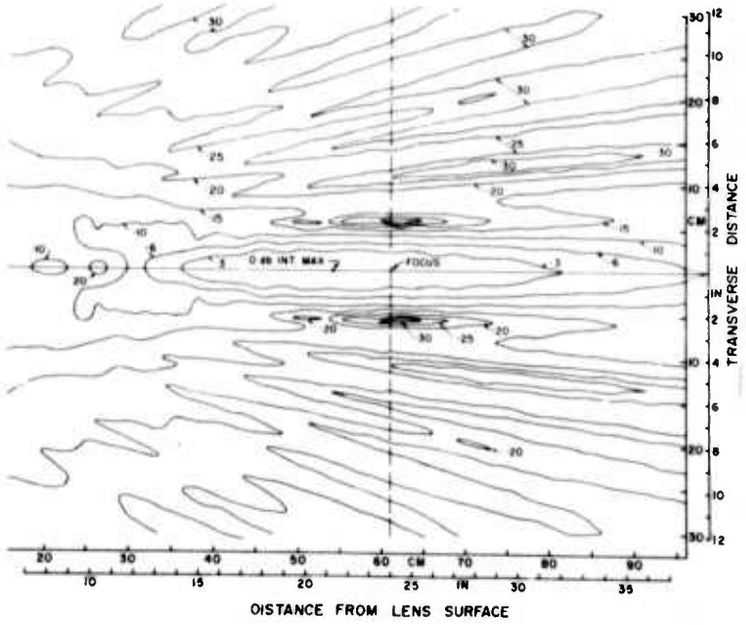

FIGURE 7 - Intensity distribution of the 19.0 in. lens.

As just indicated, the detector crystals are biased by means of the reference signal to the appropriate current level for operation as linear detectors. Under these conditions, the detector current is proportional to the field strength in the guide and,

$$I_d \sim K_d \quad V_g \tag{4}$$

where K_d is a constant of proportionality between current and voltage.

The voltage at the output of the hybrid mixer (incident upon the detector) consists of the vector sum of the reference arm signal and the transmission arm signal

$$\vec{V} = \vec{V}_r + \vec{V}_s$$

In operation, the reference signal V_r is made at least one order of magnitude greater than the transmission arm signal. Let A represent $|\vec{V}_s|$ and B represent $|\vec{V}_r|$ and let ϕ be the phase angle between $\vec{V}_r$ and $\vec{V}_s$. Then the resultant field at the detector has the magnitude

$$|\vec{V}| = (A^2 + B^2 + 2\ A\ B\ \cos(\phi))^{\frac{1}{2}} \simeq B + A\ \cos(\phi) \tag{5}$$

Suppose further that in the absence of any plasma (or electrons) in the transmission arm, we align $\vec{V}_r$ and $\vec{V}_s$ so that $\phi_o = 0$ and let the phase shift due to the introduction of a plasma in the transmission arm be $\Delta\phi$. The difference in voltage due to the addition of the phase shift is consequently

$$(\Delta|\vec{V}|)_c = A \cos(\Delta\phi) - A_o$$

and the change in diode current is

$$(\Delta I_d)_c = K_d (A \cos(\Delta\phi) - A_o) \tag{6}$$

In these last equations we have distinguished between the amplitude A_o of the reference arm signal $\vec{V}_s$ in the absence of a plasma ($\Delta\phi = 0$) and the amplitude A in the presence of plasma and phase shift (non-zero $\Delta\phi$). For low pressure weakly ionized plasmas such as encountered in the present work, $A = A_o$ and

$$(\Delta I_d)_c = K_d A_o (\cos(\Delta\phi) - 1)$$

This particular type of detection is referred to as COSINE detection.

If instead of $\phi_o = 0$ we had chosen $\phi_o = \frac{\pi}{2}$, we would have had

$$(\Delta|\vec{V}|)_s = -A \sin(\Delta\phi)$$

and

$$(\Delta I_d)_s = -K_d A \sin(\Delta\phi) \tag{7}$$

For low pressure weakly ionized plasmas, A can be replaced by A_o; thus

$$(\Delta I_d)_s = -K_d A_o \sin(\Delta\phi)$$

which will be referred to as SINE detection. For small phase shifts, it is better to operate with SINE detection.

For situations where high electron density levels are encountered or where attenuation as well as phase shift occurs in the transmission arm, both SINE and COSINE detection are required. Each detector arm is arranged to simultaneously incorporate both types of detection so that for the i_{th} channel

$$\begin{aligned} ((\Delta I_d)_c)_i &= ((K_d)_c)_i \, A_i \, \mathrm{COS}(\Delta\phi_i) - ((K_d)_c)_i \, (A_o)_i \\ ((\Delta I_d)_s)_i &= ((K_d)_s)_i \, A_i \, \mathrm{SIN}(\Delta\phi_i) \end{aligned} \tag{8}$$

where i refers to channel 1 or channel 2.

The four measurements (i = 1,2) enable one to solve for the four unknowns A_i and $\Delta\phi_i$.

In the method of recording on the DREV Range 5 interferometer, the signals are recorded from oscilloscopes using Polaroid cameras. The deflection sensitivities of the oscilloscopes are established prior to the firing by chopping the energy in the transmission arm and calibrating the sensitivity setting in terms of the amplitude A_o of the electric field in the transmission arm in the absence of any plasma. The calibration is done in the COSINE arms after ensuring $\phi_o = 0$, and in the SINE arms by removing $\frac{\pi}{2}$ radians from the value of $\phi_o = \frac{\pi}{2}$ in these arms during the calibration period. Essentially the oscilloscopes are adjusted so that a deflection on the oscilloscope screen of 5 or 10 or 20 or 40 cm represents the amplitude A_o. The procedure is fully described elsewhere (32).

According to analyses which may be found in standard texts (34), the phase shift, arising along the path of a plane wave when an electron

density function $n_e(x)$ is introduced instead of free space, is determined by

$$\Delta\phi = \int_{path}\left(1 - \left(1 - \frac{n_e(x)}{n_c}\right)^{\frac{1}{2}}\right) \frac{2\pi}{\lambda}\, dx \qquad (9)$$

$$\simeq \frac{1}{n_c} \int n_e(x)\, dx$$

provided that $\frac{n_e(x)}{n_c}$ is always less than unity. The critical electron density n_c is defined by

$$n_c = \frac{\varepsilon_o\, m\, \omega^2}{e^2} \simeq 10^{12}\ \text{cm}^{-3} \text{ at } X_s\text{-band},$$

where
- x is the distance along the path of the beam,
- ε_o is the permittivity of free space,
- m is the electron mass,
- ω is the microwave angular frequency, and
- e is the electron charge.

Substituting

$$\Delta\phi = \frac{1}{\omega}\, \frac{2\pi}{118.4} \int_{path} n_e(x)\, dx \qquad (10)$$

where x is measured in centimeters and $n_e(x)$ in cm^{-3}

To estimate electron density in a cylindrical wake, it was assumed that the appropriate distribution is gaussian. In cylindrical coordinates

$$n_e(R) = n_{eo} e^{-R^2/r^2}, \qquad o \leq r < \infty$$

Then, assuming a microwave beam passes through this distribution at a distance y from the center, we have

$$n_e(x) = n_{eo} e^{-y^2/r^2}\, e^{-x^2/r^2}$$

and

$$\int n_e(x)\ dx = \sqrt{\pi}\, n_{eo} r e^{-y^2/r^2} \tag{11}$$

Suppose now that we have two focussed microwave beams looking at a cylindrical plasma (as in the DREV Range 5 interferometer system) and suppose that the plasma has a gaussian distribution of electron charge $n_e(R) = n_{eo} e^{-R^2/r^2}$. Then if one beam traverses the cylinder at an offset distance from the axis of y_1, and the second beam traverses at an offset distance y_2, the two phase shifts occurring in the beams will be respectively

$$\Delta\phi_1 = K \sqrt{\pi}\, n_{eo} r e^{-y_1^2/r^2}$$

and

$$\Delta\phi_2 = K \sqrt{\pi}\, n_{eo} r e^{-y_2^2/r^2}$$

where $K = \frac{1}{\omega} \frac{2\pi}{118.4}$

The two parameters of the gaussian distribution of electron density n_{eo} and r, may be determined by solving these two equations in terms of the measured phase changes $\Delta\phi_1$ and $\Delta\phi_2$ and the known offset distances y_1 and y_2

Consequently

$$r^2 = (y_2^2 - y_1^2) \ln (\Delta\phi_1/\Delta\phi_2) \tag{13}$$

determines r, and subsequently

$$n_{eo} = \frac{\Delta\phi_j\, e^{-y_j^2/r^2}}{Kr\sqrt{\pi}} \tag{14}$$

for j = 1 or 2

Insofar as a gaussian distribution is appropriate for describing the electron density in the wake, a two-channel interferometer offers the possibility of determining the amplitude on the wake axis n_{eo}, as well as the radius r, at the 1/e height of the distribution.

4.0 DATA PROCESSING

4.1 Langmuir Probe Signals

In the case of the Langmuir probes, the signals are recorded in pairs on rolls of 35 millimeter film. The raw results of a trial with these probes consists of a dozen or more films, each streaked by two wiggling black lines representing probe signals. The first step in the data reduction process is to convert these recorded signals into two transparent traces on an opaque field by making a positive from the original film. This positive can then be processed by the DREV automatic film reader.

The operation of the automatic film reader has been described in detail in a recent publication (35). By means of an electro-optical system, a film transport mechanism and a digital computer, a digital representation is obtained of the probe signals recorded in analog manner on the film at a prescribed sampling frequency. (The sampling frequency can be as high as 1 MHz.) There are two sources of error in the digitalization method for which it is customary to make corrections (19). However, in the Langmuir probe experiment, these corrections are relatively unimportant, except for large axial distances, because of the high amplitude of the probe signals.

The numerical values corresponding to the sampled points of the probe signals are inscribed on a magnetic tape by the data reader. In the following step, this tape is recorded and then decoded by the XDS Sigma 7 computer facility at DREV. From this stage, the analysis

proceeds in a fashion similar to that employed in the case of the ion probe array experiments at DREV (19). First the signals are divided into consecutive segments of 0.5 millisecond duration. During 0.5 milliseconds, the projectile recedes an additional 32 body diameters from the location of the probe. To each one of the signal segments is allocated an analysis number, and the results of any analyses performed on the signal segments are assigned to an axial distance behind the projectile corresponding to the middle of the segment.

The basic operation which is invariably performed on any pair of probe signals is to cross-correlate the segment of signal from the upstream probe with that of the downstream probe (19).

$$R_j = \frac{\sum_{i=1}^{N} (x_i - \bar{x})\,(y_{i+j} - (\bar{y})_j)}{\sqrt{\overline{x^2}}\;\sqrt{(\overline{y^2})_j}} \quad , j=0, 1, 2, \ldots r \tag{15}$$

where

$$\bar{x} = \frac{1}{N}\sum_{i=1}^{N} x_i \; ; \quad (\bar{y})_j = \frac{1}{N}\sum_{i=1}^{N} y_{i+j} \tag{16}$$

$$\overline{x^2} = \frac{1}{N-1}\sum_{i=1}^{N} (x_i - \bar{x})^2, \tag{17}$$

$$(\overline{y^2})_j = \frac{1}{N-1}\sum_{i=1}^{N} (y_{i+j} - (\bar{y})_j)^2. \tag{18}$$

In these expressions x_i represents the digital trace of the upstream probe and y_i that of the downstream probe. (The expression 'digital trace' is used in preference to the term 'sampled signals'). All these data are stored on magnetic tapes. In this report the values of $\bar{x}$ and $(\bar{y})_o$ are of central interest as these can be used to obtain the mean current drawn by the various probes.

In a preceding section it was seen that the current signal detected by a probe immersed in the wake undergoes many transformations before finally ending in the form of a digital trace susceptible to manipulation on a digital computer. The transfer function between the probe signal and its digital trace is given by

$$I = \frac{(C_o - C) \cdot G}{R_F \cdot G_{AL} \cdot G_L \cdot F} \qquad (19)$$

where

I is the current collected by the probe

C_o is the zero reference level of the digital trace

C is the value (in counts) of any point on the digital trace

G is the sensitivity employed on the oscilloscope

R_F is the feedback resistor of the current to voltage preamplifier (0.2 Megohms)

G_{AL} is the gain of the line driver amplifier

G_L is the magnification factor between the screen of the oscilloscope and the 35 millimeter film in the Fastax camera (0.35)

and

F is the vertical scale factor (or frequency) in the PDP-5 automatic film reader (758 counts/centimeter)

The quantities R_F, G_L and F are universal constants in the sense that they have the same value for all recent rounds. When these are replaced by their numerical values, Equation 19 becomes.

$$I = 18.846 \left[\frac{(C_o - C) \cdot G}{G_{AL}}\right] \qquad (20)$$

where

I is now expressed in nanoamperes

C is in counts

and

G is in volts/cm.

Equation 20 is used to determine the mean current detected by a probe. The values of G and G_{AL} are determined at the time of the trial. If it is desired to calculate the mean current of the upstream probe, C is equated to $\bar{x}$, or if it is desired to calculate the mean current to the downstream probe, C is equated to $(\bar{y})_o$. In either case, the required information can be found written on magnetic tapes as previously described. The signal level C_o of the mean current is obtained as follows. In the first approximation, C_o is determined by averaging two arithmetic means. The first of these mean values is obtained by averaging over a segment of signal recorded just before the passage of the projectile (i.e. before the probe begins drawing current) and the second mean is obtained from a segment of signal corresponding to the far wake where it is reasonable to assume that the probe no longer draws any current. The two sources of error previously mentioned also affect the zero level found by the above procedure (19). Accordingly the zero level is adjusted in such a way as to minimize the effect of these errors. A list of corrections is prepared corresponding to the analysis numbers assigned to the signals, and a global correction is subsequently applied to the mean values $\bar{x}$ or $(\bar{y})_o$, previously defined.

The current drawn by a Langmuir probe immersed in a hypersonic turbulent wake decreases rapidly as the projectile recedes from the probe or vice versa. This is so much the case that it is necessary to record the probe signals at several different gains if one wishes to make measurements from just behind the projectile to several hundreds of diameters of axial distance in the wake. Given the same signal recorded at two or more gains with some obvious overlapping, it becomes necessary to undertake a certain amount of editing when attempting to determine a consistent history of the mean current collected by a given probe. As

discussed in the previous paper (19) on the deduction of ion density levels from ion probe measurements, a program makes the final selection of the segments of probe signal, keeping, for each analysis number, only the mean current which was recorded by the oscilloscope having the highest sensitivity. When the possible relative error begins to exceed the mean signal level, analyses of the probe current is terminated (19).

The calibration of all the apparatus employed in the recording of the probe signals was periodically verified. In this fashion it was possible to assure the proper functioning of the preamplifiers associated with the probes. In addition the effects of the 170 feet of cable in the terminated transmission line between the line-driver amplifiers and the oscilloscopes in the recording room were also periodically checked; the method involved sending a signal of known amplitude at a frequency of 1 kiloHertz through the system and measuring the resulting deflection on the cathode ray tube of the oscilloscope. The transmission factor of the line-driver-amplifier-terminated-line system was about 0.9. Correction for these transmission losses provides a final adjustment that must be made to the mean currents detected by the probes.

Once the final estimates of the probe currents are obtained, the electron density behavior can be calculated. From Equations 2 and 3

$$\frac{I_i}{(r_p)_i \, L_i} = 2\pi(j_e)_i = 1.90 \times 10^{-11} \, n_e (V_i - V_p)^{\frac{1}{2}} \qquad (21)$$

where

r_p is the radius of a probe

L is the length of the probe

and

I is measured in amperes,

r_p, L in centimeters

n_e in $(\text{centimeters})^{-3}$ and

V, V_p in volts.

Here i indicates the i_{th} probe. In Mode 1, two current measurements from two different probes operating at different bias voltages permit the simultaneous solution for the electron density n_e and the plasma potential V_p. In Mode 2 operation, V_p is specified and the current measurements from a single probe can be used to estimate the electron density n_e.

4.2 Interferometer SIN($\Delta\phi$) Signals

The paired interferometer signals recorded on the polaroid film were digitalized by superimposing a rectangular grid (minimum dimension of one millimeter) over the polaroids and by reading the amplitude of the signals to the nearest possible decimal of a millimeter. The periods in the signal during which the beams were gated off by the PIN modulator provided an absolute zero reference level against which both the nominal zero signal level (before the passage of the projectile) and the actual signal amplitude could be measured. The two channels were read in synchronization with the aid of gating markers. The amplitudes were corrected for the reduction factor of 0.9 of the Polaroid cameras, and the phase shifts were calculated from the arcsine functions. These phase shifts were then corrected to obtain the true phase shift by adding or subtracting, as required, the phase shift corresponding to any finite difference between the nominal zero signal level and the absolute reference level determined by gating off the beams.

These procedures were programmed for the digital computer. The tables of data representing the digitized amplitudes of the simultaneous signals on both interferometer channels were read into the computer, along with constants representing the maximum possible signal amplitude, the sweep speed, the zero level corrections, the point in time corresponding to the beginning of the signal, the position of the beams with respect to the wake axis, and the speed of the projectile. The computer consequently calculated values of the wake electron density radius r and the amplitude of the electron density n_{eo} on the wake axis as a function of the normalized axial distance X/D behind the projectile. This was done for the digitized data on each of the polaroids that were selected for analysis. Subsequently the results were plotted by the data plotter.

5.0 RESULTS

5.1 Interferometer Results

Figure 8 is a composite illustration of the signals from the two channels of the interferometer equipment, recorded at two amplifications (5 centimeter and 20 centimeter full scale deflection) and two sweep speeds (0.2 and 0.5 milliseconds/centimeter). Inside the range, the wake axis was 0.58 inch from the center of the Channel #2 beam and 2.20 inches from that of Channel #1. Thus initially behind the sphere at small axial distances, where the wake is relatively narrow, there is a large difference in the signals from the two channels. At larger axial distances where the wake becomes larger compared to the distances from the beam axes to the wake axis, the signals tend to have similar amplitudes.

In practice, the values of the electron density on the wake axis n_{eo} and the electron density radius r were found to be subject to considerable scatter. Examination of the equation defining r^2 from the known position of the beams and the relative phase shifts detected in the

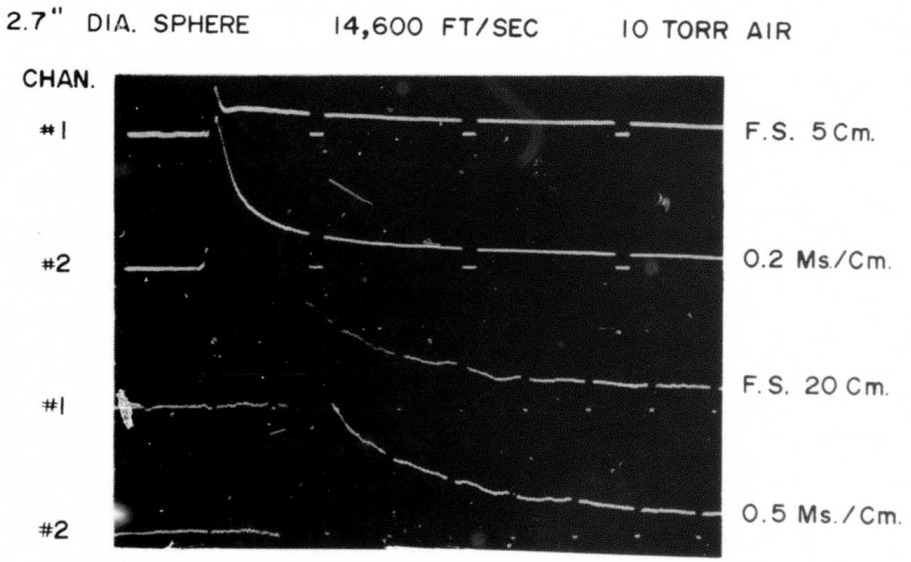

FIGURE 8 - Dual channel interferometer signals.

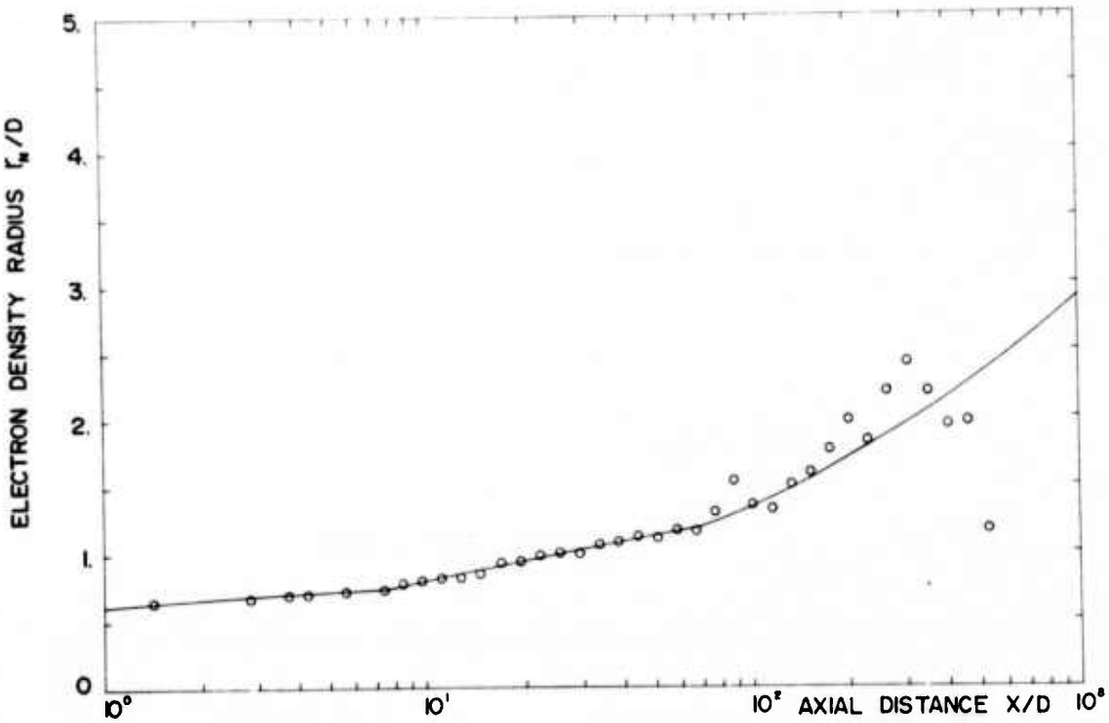

FIGURE 9 - Electron density radius r/D as a function of X/D.

two channels shows that the equation is very nonlinear. When y_1 and y_2 are not greatly different, the phase shifts $\Delta\phi_1$ and $\Delta\phi_2$ tend to become equal at some axial distance behind the projectile. Fluctuations or reading error in one or both of these quantities lead to scatter in the estimated values of r and n_{eo}. (Under these conditions it is possible for the formula to indicate a negative value of r^2. When this happens, the solution is rejected and the computer proceeds to the next pair of points).

The scatter just described made it difficult to compare the results of various rounds. Accordingly a selection of radius data was made amongst the various rounds and averaged to obtain the mean electron density radius curve r/D shown in Figure 9. This curve was fitted piece-wise by the following analytical expressions

$$r/D = 0.62 + 0.137 \log_{10} (X/D) \quad \text{for } 1 \leq X/D \leq 7.5$$

$$= 0.325 + 0.475 \log_{10} (X/D) \quad \text{for } 7.5 \leq X/D \leq 70 \qquad (22)$$

$$= 0.291 (X/D)^{1/3} \quad \text{for } 70 \leq X/D \leq 1000$$

The first two expressions represent an excellent approximation to the radius estimates. In the third region of axial distance, a one-third power law was chosen to represent the highly scattered results.

This analytical expression for the experimentally determined average radius of the assumed gaussian electron density distribution of the wake was introduced into Equation 14 and the equation solved for the value of the electron density on the wake axis. With the wake radius prescribed, each channel of the interferometer will give an independent estimate of the behavior of the parameter n_{eo} as a function of axial distance. Through the use of this prescribed radius technique, it was found possible to collapse much of the data and to clearly differentiate between 'clean' and 'dirty' rounds (36).

(The adjective 'dirty' is a colloquial term which implies that there seems to be an excess of signal beyond the amplitude of the signals normally observed, and that there are possible fluctuations or bumps superimposed on the generally smooth decay of the signal amplitude observed with the interferometer as the axial distance behind the projectile increases. Of course abnormally large signals imply an excess of ionization and this is usually attributed to dirt or impurities in the range atmosphere. A dirty range atmosphere is often blamed for what has come to be called a 'dirty round', although similar effects are observed if the projectile is

damaged or accompanied down the range by broken and ablating pieces of the plastic sabot (36).)

Figure 10 shows the electron density on the wake axis estimated from the signals measured on one of the interferometer channels on a 2.7 inch diameter sphere firing at 10 torr. The different symbols come from different polaroid recordings: the circles, diamonds, and squares from 5, 20 and 20 centimeter full scale amplitude recordings with sweep speeds of 0.2, 0.5, and 1.0 milliseconds/centimeter respectively.

The mean smoothed curve of the electron density data on the wake axis has been obtained from a number of clean rounds similar to that shown in Figure 10. These mean curves were found to lie in the shaded region shown in Figure 11, which represents the results from five different rounds and ten independent channel measurements. A conclusion of major importance from Figure 11 is that it is possible to obtain reproducible electron density measurements under the normal operating conditions in the DREV Range 5 (36).

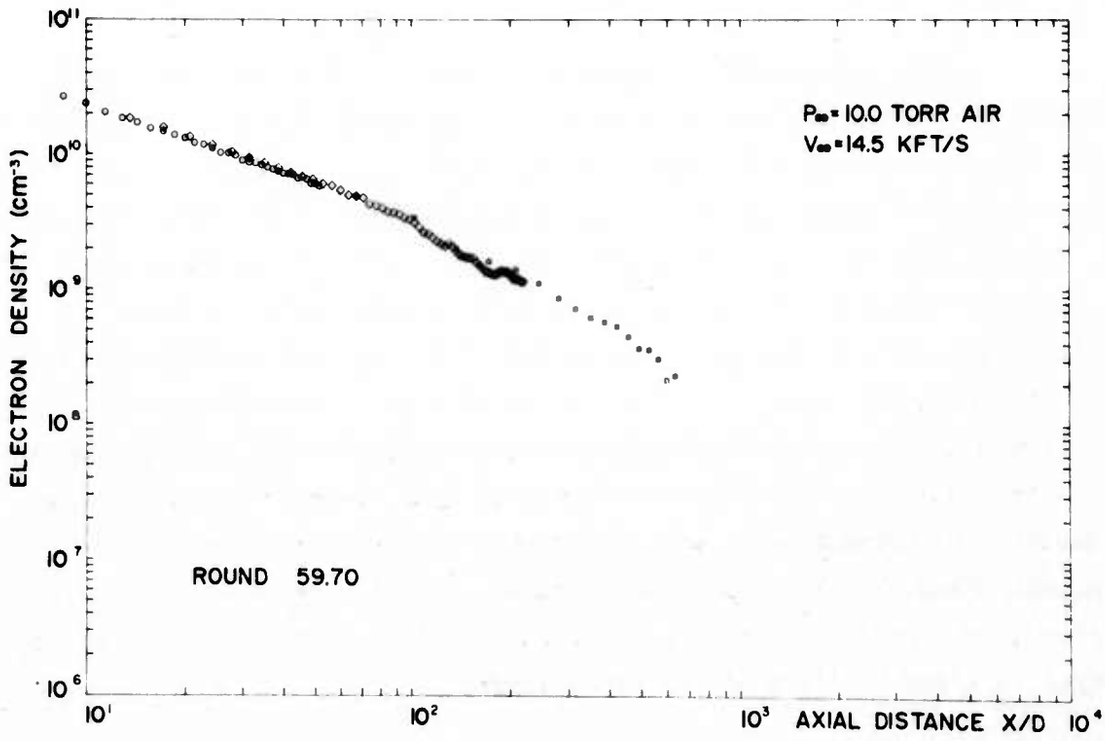

FIGURE 10 - Electron density on the wake axis deduced from the dual channel interferometer.

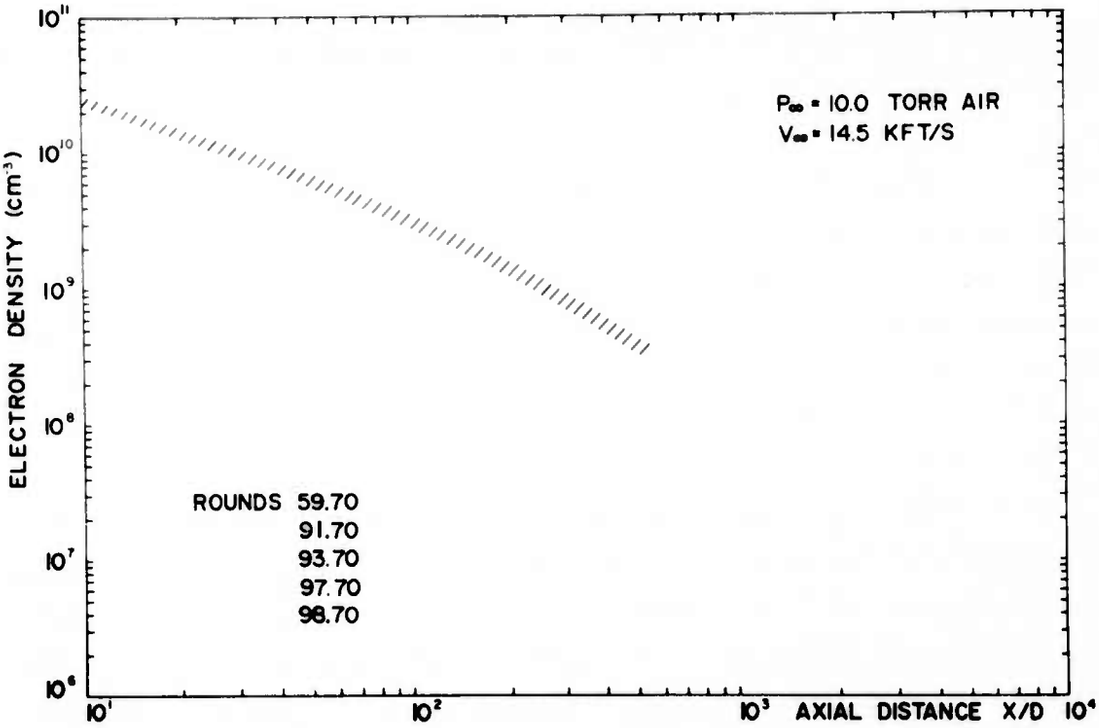

FIGURE 11 - Consistency of interferometer electron density data on 'clean' rounds.

5.2 Langmuir Probe Results

The total firing program for the Langmuir probe experiment, including development rounds, consisted of about 26 firings. While this may seem like a relatively small number, it still represents a large fraction of the total number of rounds (approximately 90 - 100) that can be launched in one year on the DREV Range 5. Subtracting development rounds and bad rounds where the projectile was damaged or followed by sabot fragments, we have a net number of 13 firings where useful data was obtained, of which 10 were in air at 10 torr. Imposition of the criterion that the interferometer electron density result be reproduced to within 25%, reduced the above number to about eight acceptable rounds. Finally, for present purposes, this number was further reduced by including analyses from only those rounds where the probe wires survived after re-entry of air into the range and could be photographed so as to permit a close estimate of the probe length.

The gap between the open ends of the ceramic tubing was measured with respect to a calibrated scale on an enlargement of a photograph taken before the firing. From an enlargement of a photograph taken subsequent to the firing, the length of the probe wire was measured by comparison to this gap, including correction for any curvature in the wire. At the beginning, the wires were photographed from only one direction. The average correction, or the excess of the probe length over the width of the gap was about 5%. Later the wires were photographed both horizontally and from above, and the largest of the corrections obtained from these two directions was applied.

Samples of the wires were also measured by a powerful optical microscope. The diameter of the probe wires was found to be fairly constant and close to the nominal value of the manufacturer. In one case the wire diameter was found to be undersize, presumably from yielding under tension while being heated by the plasma scrubber.

Figure 12a shows a typical set of signals obtained from four Langmuir probes in the wake of a 2.7 inch diameter sphere flown at 14,600 feet/second in a 10 torr air atmosphere. In turn, from the first and upstream probe, the probe biases were 2, 2.5, 3 and 3.5 volts. The signals from the first two probes with the weakest bias voltages are shown at twice the amplification used to record the signals of the two more strongly biased probes. As seen from Figure 11, the amplitudes of the signals obtained from the probes biased at 3 and 3.5 volts are comparable, and both are considerably larger than that obtained by the probe with 2.5 volts bias. The weakly biased upstream probe attracts a current which rapidly disappears. Figure 12b shows signals obtained from four Langmuir probes biased at 9 volts.

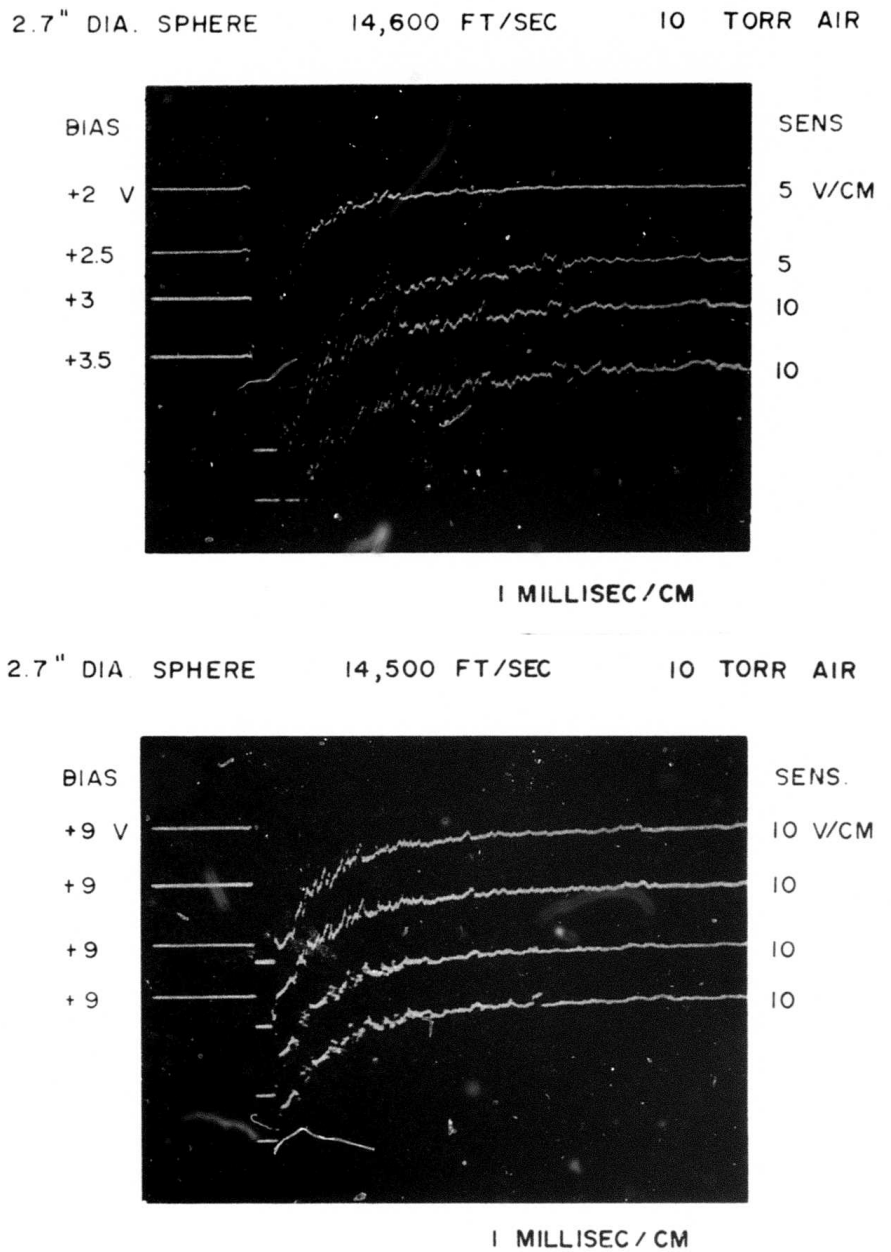

FIGURE 12 - Typical Langmuir probe array signals from Mode 1 (a) and Mode 2 (b) operation.

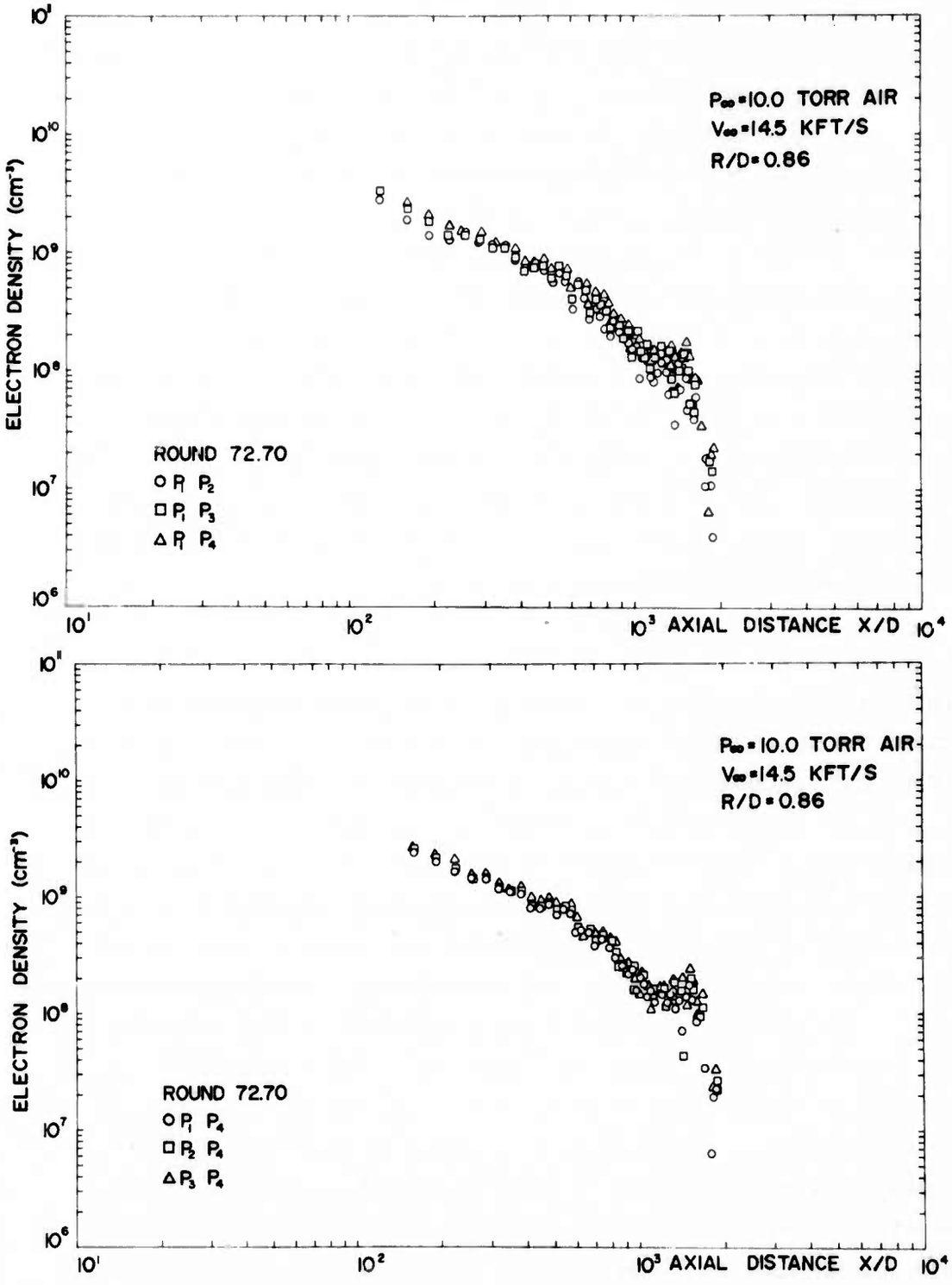

FIGURE 13 - Electron density estimates obtained from the analysis of signals of various combinations of Langmuir probes on a Mode 1 trial. The bias of the probes were as follows: P_1, 2.5 volts; P_2, 3 volts; P_3, 3.5 volts; and finally P_4, 4 volts.

Such signals were digitalized from the 35 millimeter Fastax film recordings and analyzed as previously described. At this juncture it is well to remark that the configuration of Langmuir probes employed in this work was more appropriate for the estimation of turbulent scales than for tne estimation of electron density. The probes of any given pair of probes are located not at the same point in the wake but are separated by multiples of 0.5 inch. Necessarily, the solution of Equation 21 for the parameters n_e and V_p will result in numerical estimates, but while these estimates are representative of conditions in the wake at a given set of radial and axial distance coordinates, they cannot be strictly attributed to a specific point in the fluid. (For this reason, the values of statistical parameters representing the fluctuating properties of the electron density in the wake are derived from the digital traces of the probe current (37)).

Figure 13 shows the electron density estimates derived by analyzing the signals from various pairs of probes obtained during a sphere firing at 14,500 feet/second in 10 torr air. Here probes of 0.0005 inch diameter and 4 millimeter length were operated at biases of 2.5, 3, 3.5 and 4 volts respectively for the first (P_1), second (P_2), third (P_3) and fourth (P_4) probes. In Figure 13a, the signal of the first probe (having the lowest bias voltage) is analyzed in turn with the signals of each of the other three (more highly biased) probes. There is a marked tendency for the electron density estimate from a given pair of probes to be higher when the bias of the second probe (other than the first probe) is higher. In Figure 13b, the signal of the last and most highly biased probe is analyzed in turn with the signals from all the other probes. Again, there is a tendency for the probes with the highest bias voltage to give a slightly higher estimate of electron density, although the spread between the various data points is smaller than was the case in Figure 13a. It should be noted that if the data from the probe pairs P_1P_2 in Figure 13a and P_1P_4 in Figure 13b are ignored, the spread in each figure is considerably reduced. Accordingly, the data concerning electron density to be presented later in this report will be derived from the analysis of the signals of the pairs of probes having the highest bias, which was normally P_3P_4 when Mode 1 was employed.

The estimates of the plasma potential V_p which were derived simultaneously with the electron density estimates in Figure 13b are shown in Figure 14a. It seems likely that a considerable proportion of the scatter in the data can be attributed to the fact that the two probes are not in the same ionized particle of fluid, so that the actual ionization seen by one probe at any time frequently differs from that seen by the other probe. The analysis technique, however, forces a single estimate to be derived for the electron density, and this must be reflected in the estimates predicted for the plasma potential. The plasma potential may in fact be fluctuating to some degree, but the reader must be warned that the fluctuation in the derived plasma potential shown in Figure 14 is greatly influenced by the analysis technique employed. The scatter of the data in Figure 14b where the biases of the probes were 2, 2.5, 3 and 3.5 volts respectively is somewhat less then in Figure 14a.

The conclusions that can be drawn from Figure 14 are interesting. Generally, over the range of the bias potentials employed, the results indicate that the plasma potential tended to rise towards the potential of the most highly biased probes, rather than be held near zero volts by the large grounded reference grid. Consider Figure 14b, where the trends are reasonably clear. Each set of estimates of the plasma potential V_p obtained from a different pair of probes is different; each set indicates that the plasma potential is approaching the potential of that probe of the pair which has the lowest bias voltage. For the more weakly biased probes where the current tends to become zero at a few hundred diameters behind the sphere, Equation 21 shows that this result is inevitable: as soon as the current drawn by the more weakly biased probe approaches zero, the solution of the equations demands that the value of V_p be equal to the bias potential of that probe. Again the best estimate of the behavior of the average value of the plasma potential must be attributed to the pair of probes with the highest minimum value for the probe bias voltage. Figure 14 indicates that the plasma potential tends to assume a value within 0.5 to 1 volt of the bias potential. This will lower the actual value of the normalized plasma potential ϕ^* used in the experiment below that shown in Figure 1 (based on a difference of 2 volts between

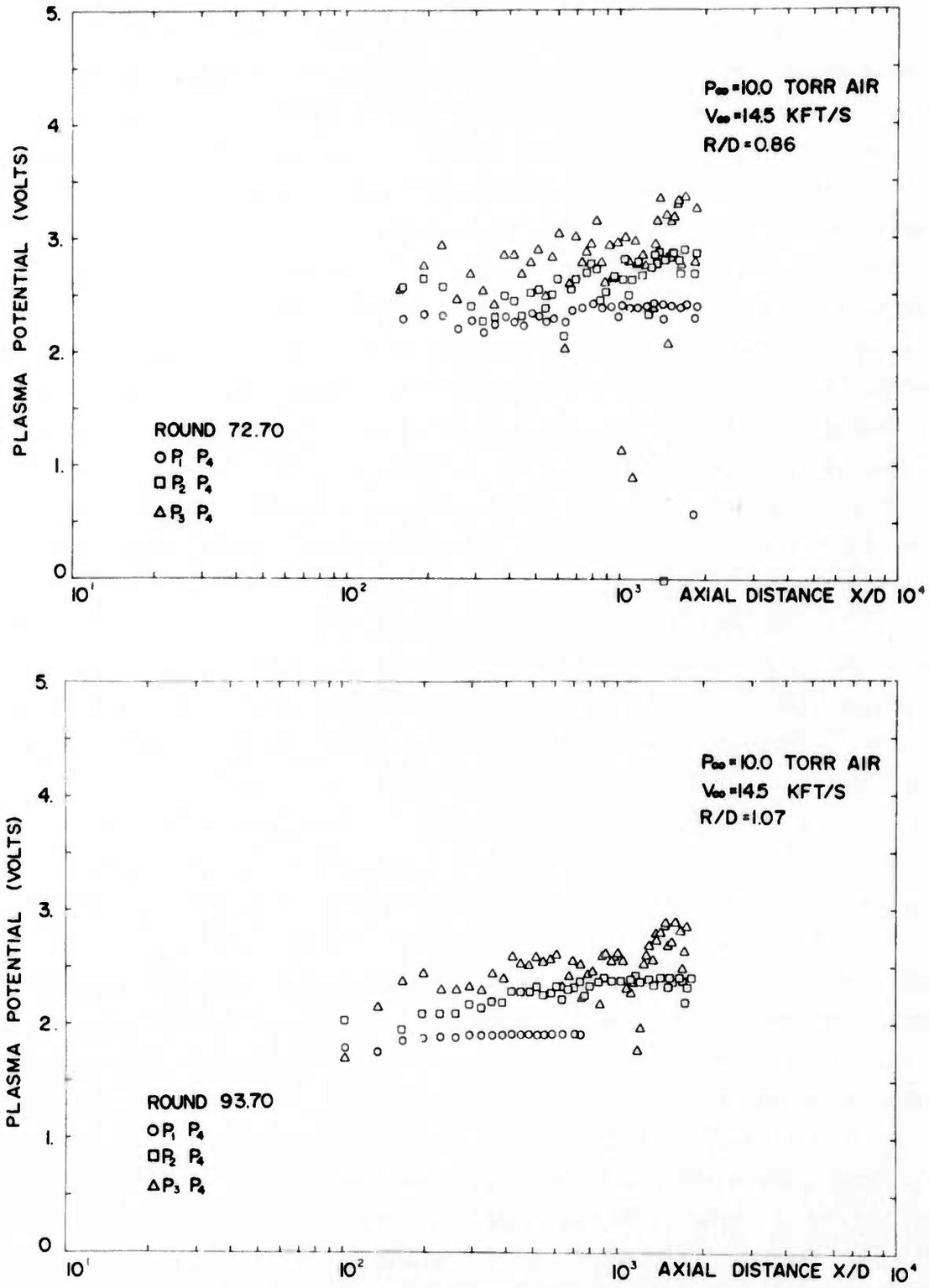

FIGURE 14 - Plasma potential behavior as deduced from analysis of Langmuir probe signals, showing the dependence of the estimate of the plasma potential on the bias voltages of the probes.

the probe and plasma potentials). However, the assumption $\phi^* \gtrsim 10$ is still generally satisfied for the most positively biased probes over the range of axial distance for which data is presented.

Let us now look at the consistency of some of the electron density estimates obtained with the Langmuir probes. Figure 15a shows a comparison of data from two rounds fired in 10 torr air atmospheres which passed approximately the same radial distance away from the probes. The interferometer results here represent estimates of the electron density on the wake axis, while the probe results estimate the electron density at the indicated radial distance. On both of these rounds the length of the probe wires was about 4 millimeters; in the case of Round 72 the wire diameter was 0.0005 inch and the biases ranged from 2.5 to 4 volts, while for Round 91 the wire diameter was 0.001 inch and the biases ranged from 2 to 3.5 volts. The interferometer data for Round 72 indicated that the electron density was about 25% higher than that for Round 91 (Figure 11); the Langmuir probe data mirrors this difference. Figure 15b compares two rounds at slightly different pressures. Here only the standard interferometer result (Figure 11) is shown, but the differences in the Langmuir probe data are in the proper direction. (For both rounds, probe lengths were 4 millimeters, diameters were 0.001 inch and biases ranged from 2 to 3.5 volts).

Figure 16 presents an interesting comparison of data from three different Rounds. In the case of Rounds 91 and 93, the probe lengths were 4 millimeters, the diameters were 0.001 inch, and the biases ranged from 2 to 3.5 volts. The probes used in Round 59 had the same diameter, but the lengths were 2.4 millimeters and all probes were biased at 3.5 volts (Mode 2). Accordingly it was necessary to assume some value for the effective plasma potential in the case of Round 59 and, based on the plasma potential data derived from other rounds where a maximum bias of 3.5 volts had been used, it was decided to use

$$V_p = 1.667 + 0.33 \log_{10} X/D \quad \text{volts} \qquad (23)$$

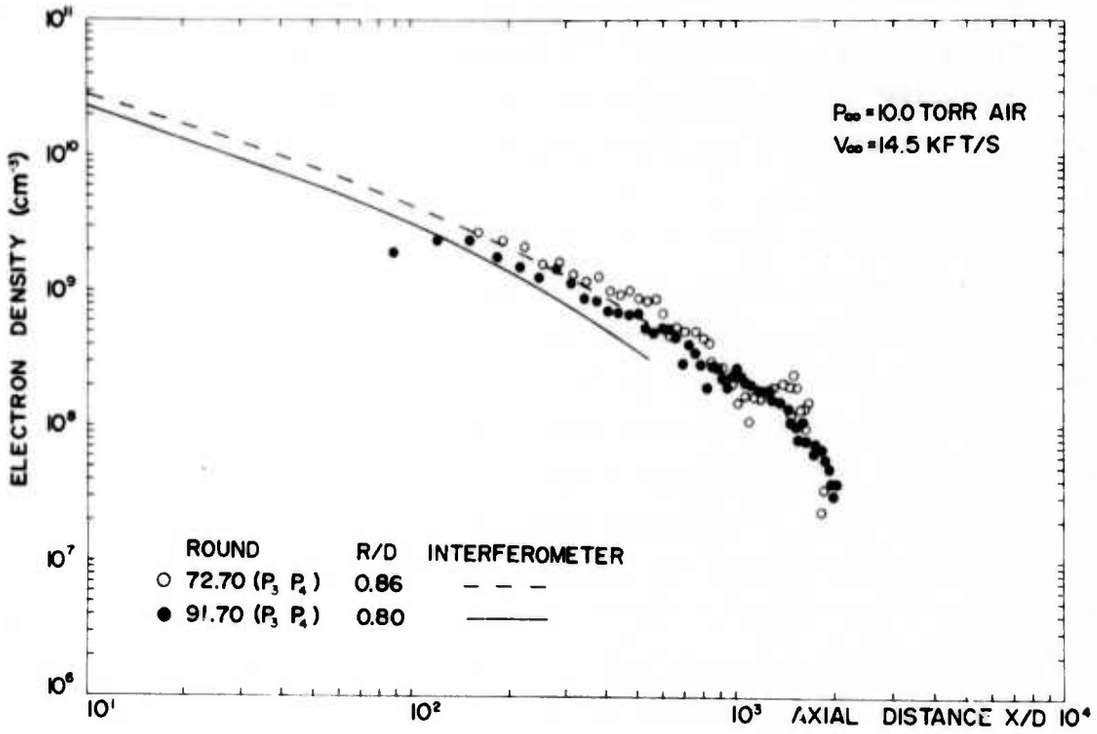

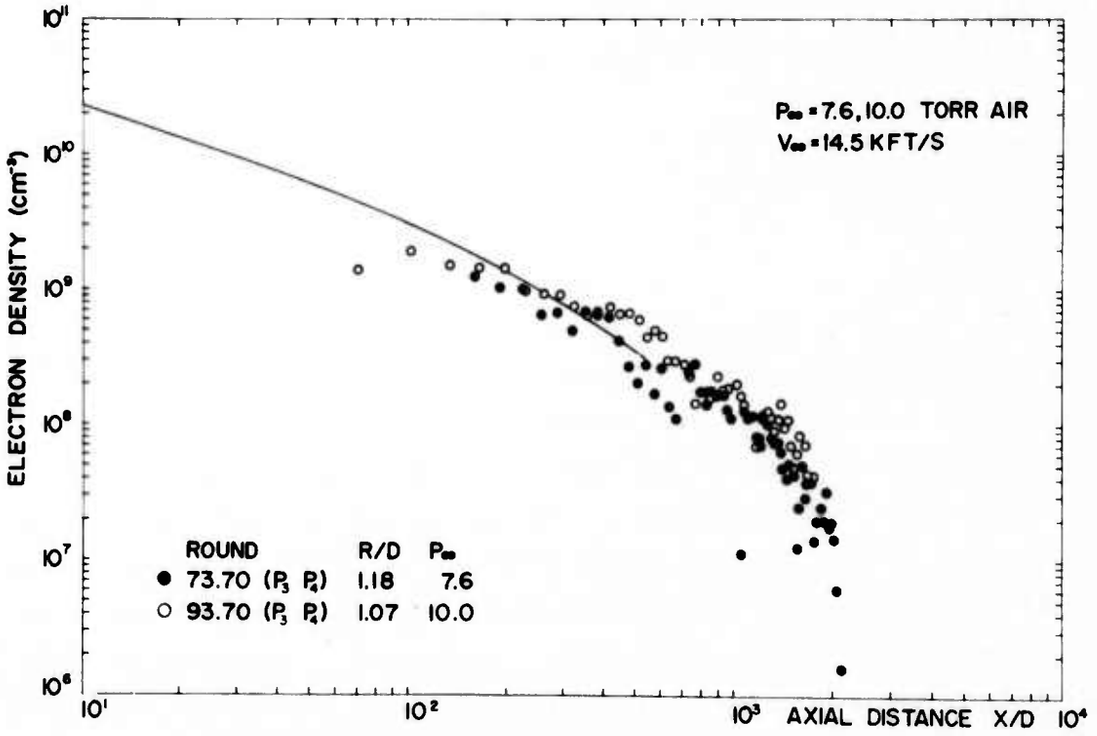

FIGURE 15 - Consistency of Langmuir probe data.

which varies from a value of 2.33 volts at X/D 100 to a value of 3.0 volts at X/D = 10,000. All the probes of Round 59 thus predicted the same behavior, which is shown in Figure 16 for the upstream probe P_1. It can be seen that the consistency of the Langmuir probe data in Figure 16 is quite excellent.

The additional dashed curve shown in Figure 16 is the result for the average wake electron density obtained in the flow field calculations carried out at AVCO to demonstrate the feasibility of Langmuir probe measurements. Since the DREV Langmuir probe data are obtained relatively near the wake axis and the AVCO electron density is an average over the whole wake, one would expect the AVCO curve to lie below the experimental data. However, the AVCO results were computed for a velocity

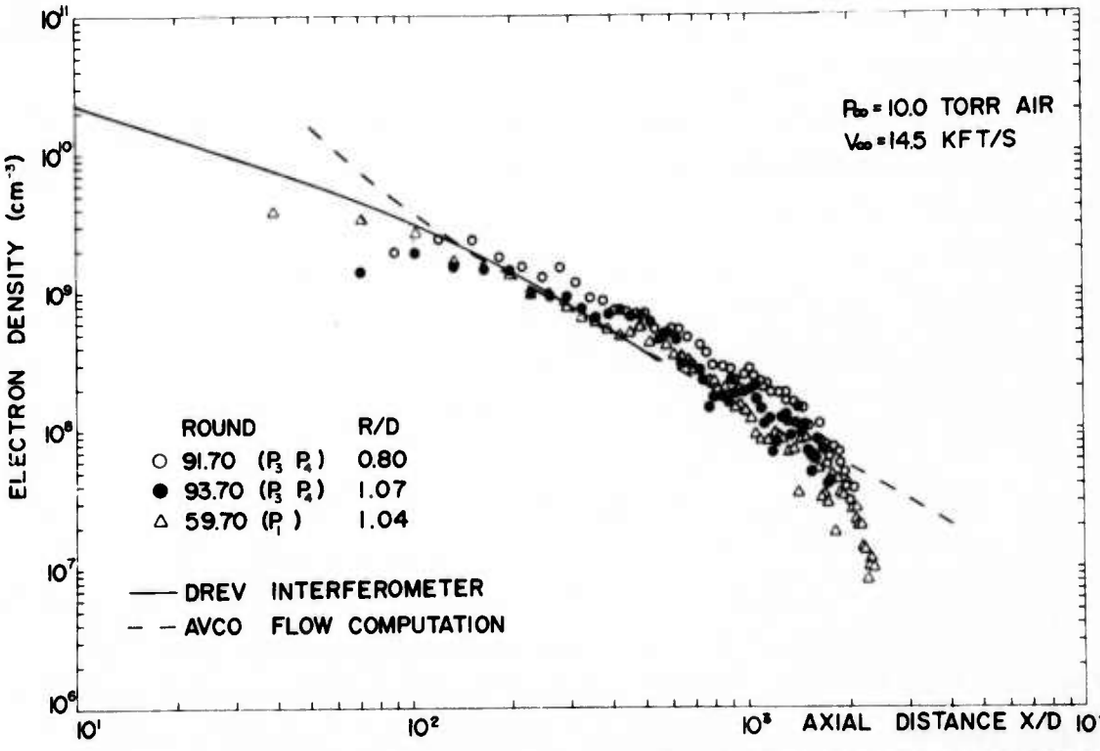

FIGURE 16 - Comparison of the Langmuir probe electron density estimates from three 'clean' rounds with the electron density estimates from the interferometer and with the average electron density predicted by the AVCO flow field calculations.

of 15,500 feet/second instead of 14,500 feet/second and based on the results of Primich and Hyami (1), this would increase the AVCO result by a factor of about 2. Another point is that the AVCO electron density is averaged over a volume defined by the schlieren radius of the wake. The DREV results (19, 36) indicate ionization radii for ions and electrons which are smaller than the schlieren radius, at least over the first few hundred diameters behind the sphere. Adjustment for this last conclusion would probably tend to increase the AVCO electron density estimates above the curve shown in Figure 16 over the first few hundred diameters.

Figure 17 presents further data confirming previous conclusions concerning the behavior of the plasma potential V_p. Both Round 97 and 98 were Mode 2 firings for turbulent scale data; both used 2.3 millimeter length probes, 0.0005 inch diameters, and in both cases all probes were biased at 9 volts. The squares in Figure 17 indicate the results obtained when the data were analyzed using Equation 23 which assumes the plasma potential varies between 2.3 volts at X/D = 100 and 3 volts at X/D = 10,000. Again the standard interferometer curve for the electron density on the wake axis is shown (Figure 11). The probe electron density estimates so derived fall considerably below the previous probe results. An explanation was sought in the possible anomalous behavior of the plasma potential. The circles show the new electron density estimates obtained when the plasma potential was assumed to follow a behavior given by

$$V_p = 7.167 + 0.33 \log_{10} X/D \qquad (24)$$

which indicates V_p = 7.83 volts at X/D = 100 and 8.5 volts at X/D = 10,000. The difference between the probe voltage of 9 volts and the plasma potential was thus between 1 and 0.5 volts over the range of axial distance of major interest, as it was in the case of the rounds where a maximum potential of 3.5 volts was employed. Since the interferometer results (Figure 11) indicated a normal behavior for Rounds 97 and 98, we believe that some automatic adjustment of the plasma potential approximately as indicated by Equation 24 is the basis of the explanation of the behavior observed on these two rounds.

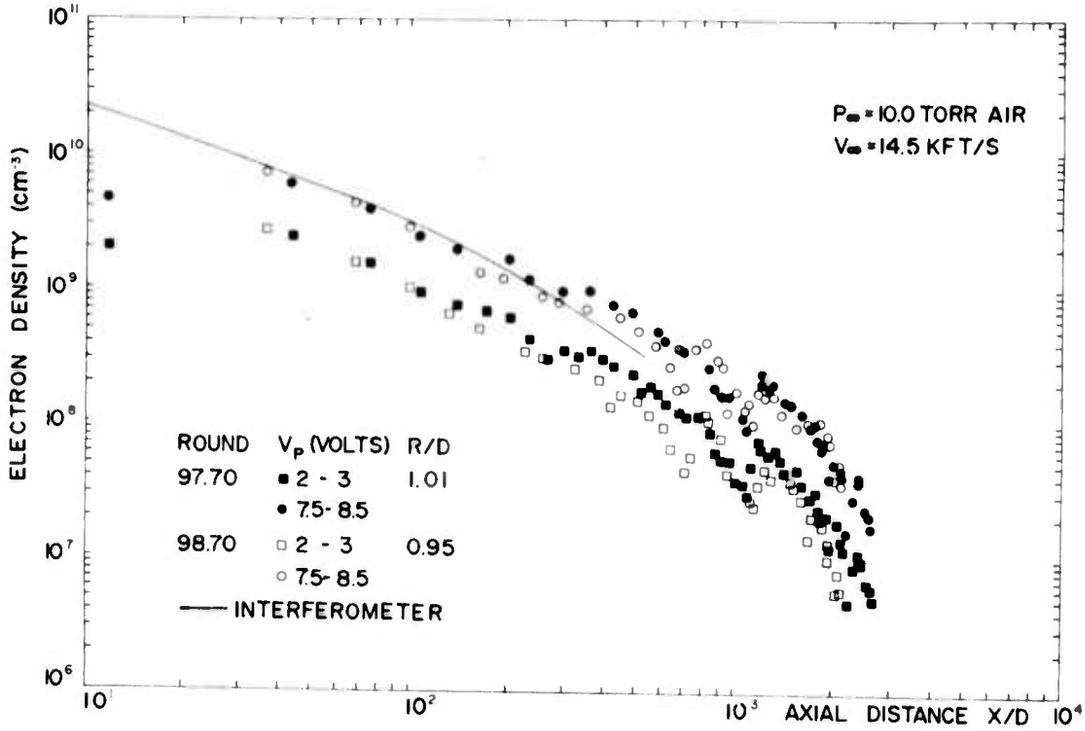

FIGURE 17 - Evidence that the plasma potential tends to lie within 1 - 0.5 volts of the probe bias voltage in the present measurements. The bias of the probes in these two rounds was 9 volts. If the plasma potential is taken to be between 7.5 and 8.5 volts, the results agree with the interferometer data and with previous results.

6.0 DISCUSSION

Despite the relative paucity of the data, the Langmuir probe electron density measurements presented in this paper are sufficiently self-consistent and sufficiently in agreement with simultaneous microwave interferometer electron density estimates as to inspire a fair degree of confidence in the results.

The method of analysis adapted for Mode 1 operation assumed that both probes of a given pair were immersed in the same ionized particle of fluid. In actual fact the disposition of the probes was chosen to favour the measurement of space correlations of electron density fluctuations, rather than the measurement of absolute electron density. The results of this compromise appear particularly evident in the scatter of the estimates of the plasma potential which are plotted on a linear scale, in contrast to the logarithmic scale used to trace the electron density results. It would be interesting to repeat the measurements with pairs of probes located closer together, although it would be necessary to avoid any possible overlapping of the probe sheaths.

The apparent agreement of the theoretical AVCO electron density results with the present measurements should be considered from the point of view of the theoretician seeking verification of his computational model, rather than from that of the experimentalist seeking support for his measurements. The computational model includes a number of gross assumptions such as that of a uniform or rectangular distribution of physical quantities across the wake and the use of the schlieren radius to define a universal wake width. In fact, as the measurements at DREV have shown, the radial distributions of various quantities in the wake are peaked and their widths differ from one quantity to another (38 - 39). Despite these factors the AVCO theoretical curve seems to be in reasonable agreement with the experimental data.

The fact that the plasma potential apparently rises toward the maximum probe bias potential was a surprise that is not yet understood. The reference or ion-collecting grid contains about 24,000 millimeters of wire which is about 1500 times the maximum total length of 16 millimeters of the 4 active electron-collecting probes when each probe has a length equal to 4 millimeters. A study of the effect of the relative size of the reference electrode on a Langmuir probe measurement has recently been published for the collisionless case by Szuszczewicz (40). Comparison with his curves indicates that the reference electrode aera to probe area ratio employed at DREV should have been sufficient to avoid problems of the reference electrode potential shifting with respect to the plasma potential and presumably the converse situation. Furthermore, the ion current for the DREV conditions was undoubtedly enhanced by ion convection by the mean flow velocity of the wake past the probes. One possibility is that the effective ion flux upon the reference grid electrode was reduced by orientation of the grid in a direction parallel to rather then perpendicular to the wake axis. The initial orientation of the grid during the early trials was perpendicular to the axis; one end was at the same radial position as the probes, and the grid extended from this towards larger radial distances. Consequently most of the reference electrode was in a region where the ion density was small and, upon some indication of limiting on the electron probe currents, the grid was installed in its present position, parallel to the axis and at the same radial distance. There is some evidence that the ion density distribution is narrower than the electron density distribution (19) based on a comparison of the electron density radii deduced from the microwave interferometer measurements (Figure 9) and the ion density radii deduced from arrays of ion probes. (The vastly different resolutions of the two techniques calls for caution in dealing with these results, however). An effort to further increase the size of the reference grid and the effectiveness of its orientation seems to be indicated, in order to maintain a higher potential difference between the electron

probes and the plasma. This is necessary to ensure the relative suppression of fluctuations in the probe current caused by possible fluctuations in the plasma potential.

Assuming such efforts were successful, possibly the most interesting application of the present Langmuir probe apparatus would be for the investigation of the space-time correlations of the electron density fluctuations in the hypersonic wake (41 -45), preferably with one or two additional probes. By maintaining the present axial resolution and collecting a reasonably large sample of results under the same ambient conditions and at the same radial distances, casting these results in the appropriate non-dimensional form and ensemble averaging over results at a given radial distance and axial distance, it should be possible to obtain an estimate of the average behavior of the space-time correlation functions at various points in the wake. However, a large effort would be required: probably one year on the DREV Range 5 facility. Such an effort is not presently contemplated.

7.0 CONCLUSION

Measurements have been carried out in the ballistic range facilities at DREV of the absolute electron density levels in the wakes of 2.7 inch diameter spheres flown at 14,500 feet/second in air atmospheres at 10 torr. The experimental technique involved the use of Langmuir probes, following the theoretical demonstration of the feasibility of such an experiment by G.W. Sutton. Considerable attention was paid to details of the experiment, such as probe cleanliness, minimum flow disturbance and the minimization of reflected shocks. Electron density level estimates obtained with the Langmuir probes were in agreement with electron density estimates derived from simultaneous measurements with a microwave interferometer. The behavior of the plasma potential in the wake was also determined; the plasma potential apparently attempted to maintain itself close to the potential of the most highly biased probes, but the reason for this behavior has not been established.

8.0 ACKNOWLEDGEMENTS

The authors are grateful to Mr. G.H. Tidy and Dr. A. Lemay, former directors of the Aerophysics Division for their interest and their support of these experiments.

The authors are indebted to Mr. P. Caron and Mme Carole Drolet for their enormous effort in the digitalization and analysis of the probe data, to Messrs P. Guay and F. Devereux for their support during range operations, to Messrs F. Leclerc and J. Williams for their assistance with respect to mechanical aspects of the experiment, and to Mr. Roger Bell, Mme M.P. Kirkwood, Mlle N. Bérubé, and Mme C. Bigras who participated in the preparation of the material for this report.

This research was jointly sponsored by the Defence Research Establishment Valcartier and by the Advanced Research Projects Agency under ARPA Order 133.

REFERENCES

1. Hayami, R. and Primich, R., "Integrated electron density in the near wakes of hypersonic velocity spheres", GM Defense Research Laboratories, TR64-01 F, May 1965 (Unclassified)

2. Kornegay, W., "Electron density decay in wakes", AIAA Journal, Vol. 3, No. 10, pp. 1819-23, October 1965.

3. Hayami, R. and Primich, R., "Wake electron density measurements behind hypersonic spheres and cones", AGARD Conference Proceedings No. 19 of the Specialists' Meeting on the Fluid Physics of Hypersonic Wakes, Colorado State University, Fort Collins, Colorado, 10-12 May 1967.

4. Guthart, H., Weissman, D. and Morita, T., "Measurements of the charged particles of an equilibrium turbulent plasma", Physics of Fluids, Vol. 9, No. 9, pp. 1766-72, September 1966.

5. Granatstein, V.L., "Structure of wind-driven plasma turbulence as resolved by continuum ion probes", Physics of Fluids, Vol. 10, No. 6, pp. 1236-44, June 1967.

6. Slattery, R.E., Clay, W.G. and Herrman, J., "Gas and electron density fluctuations in a weakly ionized hypersonic wake", Proceedings of the Symposium on Turbulence of Fluids and Plasmas, MRI Symposium Proceedings, Vol. 18, Polytechnic Press, New York, 1968.

7. Sutton, G.W., "On the feasibility of using a Langmuir probe to measure electron densities in turbulent hypersonic wakes", AIAA Journal, Vol. 7, No. 2, pp. 193-199, February 1969.

8. Heckman, D., Emond, A., Fitchett, A. and Sévigny, L., "Mean and fluctuating charge density measurements in turbulent hypersonic sphere wakes", ICIASF'71 Record, 71-C-33 AES, pp. 68-79, presented to the 4th International Congress on Instrumentation in Aerospace Simulation Facilities, held at the Von Karman Institute, Rhode-Saint-Genèse, 21-23 June 1971.

9. Fox, J. and Rungaldier, H., "Electron density fluctuation measurements in projectile wakes", AIAA Journal, Vol. 10, No. 6, pp. 790-795, June 1972.

10. Lees, L. and Hromas, L.A., "Turbulent diffusion in the wake of a blunt-nosed body at hypersonic speeds", Journal Aerospace Sciences, Vol. 29, No. 8, pp. 976-993, August 1962.

11. Zeiberg, S.L. and Bleich, G.D., "Finite-difference calculation of hypersonic wakes", AIAA Journal, Vol. 2, No. 8, pp. 1396-1402, August 1964.

12. Lykoudis, P.S., "A review of hypersonic wake studies", AIAA Journal, Vol. 4, No. 4, pp. 577-590, April 1966 (see also RAND/RM-4493 ARPA, April 1965 (Unclassified)).

13. Webb, W.H. and Hromas, L.A., "Turbulent diffusion of a reacting wake", AIAA Journal, Vol. 3, No. 5, pp 826-836, May 1965.

14. Wen, K.S., Chen, T. and Lieu, B., "A theoretical study of hypersonic sphere wakes in air and comparisons with experiments. Part I - Turbulent Diffusion. Part II - Chemical Kinetics", AIAA Paper No. 68-703 presented to the AIAA Fluid and Plasma Dynamics Conference, Los Angeles, California, 24-26 June 1968.

15. Sutton, E.A., "The chemistry of electrons in pure air hypersonic wakes", AIAA Journal, Vol. 6, No. 10, pp. 1873-82, October 1968.

16. Menkes, J., "Scattering of radar waves by an underdense turbulent plasma", AIAA Journal, Vol. 2, No. 6, pp. 1154-56, June 1964.

17. Lin, S.C., "Spectral characterization of dielectric constant fluctuation in hypersonic wake plasmas", AIAA Journal, Vol. 7, No. 10, pp. 1853-61, October 1969.

18. Guthart, H. and Graft, K.A.. "Scattering from a turbulent plasma", Radio Science, Vol. 5, No. 7, pp. 1099-1118, July 1970.

19. Sévigny, L., Heckman, D. and Caron, P., "Ion density measurements in the wake of a hypersonic sphere". Canadian Journal of Physics, Vol. 50, No. 12, pp. 2970-90, December 1972.

20. French, I.P., Arnold, T.E. and Hayami, R.A., "Ion distributions in nitrogen and air wakes behind hypersonic spheres", AIAA Paper No. 70-87, presented to the AIAA 8th Aerospace Sciences Meeting, New York, 19-21 January 1970.

21. French, I.P., Hayami, R.A., Arnold, T.E., Steinberg, M., Appleton, J.P. and Sonin, A.A., "Calibration and use of spherical and cylindrical electrostatic probes for hypersonic wake studies", General Motors AC-DRL TR69-12, May 1970 (Unclassified).

22. Demetriades, A. and Doughman, E., "Langmuir probe diagnostics of turbulent plasmas", AIAA Journal, Vol. 4, No. 3, pp. 451-459, March 1966.

23. Langmuir, I. and Mott-Smith, H.M., "The theory of collectors in gaseous discharges", Phys. Rev., Vol. 29, No. 4, pp. 727-763, October 1926.

24. Laframboise, J., "Theory of spherical and cylindrical Langmuir probes in a collisionless, Maxwelliam plasma at rest", UTIAS Rept. 100, Institute for Aerospace Studies, University of Toronto, June 1966.

25. Kirkpatrick, A., Heckman, D. and Cantin, A., "Wake plasma turbulence study using an electrostatic probe array", AIAA Journal, Vol. 5, No. 8, pp. 1494-95, August 1967.

26. Heckman, D., Williams, J., Robertson, W., Podesto, B. and Emond, A., "Summary report on the attenuation of reflected shocks in DREV ballistic range facilities", DREV R-675/73, January 1973 (Unclassified).

27. Ghosh, A.K. and Richard, C., "Probe geometry effect on turbulent plasma diagnostics", RCA Victor Company Ltd., Research Laboratories Report No. 3.900.12, May 1968 (Unclassified).

28. Wehner, G. and Medicus, G., "Reliability of probe measurements in hot cathode gas diodes", Journal Applied Physics, Vol. 23, No. 9, pp. 1035-46, September 1952.

29. Persson, K.-B., "Brush cathode plasma - a wall-behaved plasma". Journal Applied Physics, Vol. 36, No. 10, pp. 3086-94, October 1965.

30. Musal, H.M., "An inverse brush cathode for the negative-glow plasma-source", Journal Applied Physics, Vol. 37, No. 4, pp. 1935-37, March 1966.

31. Thomas, T.L. and Battle, E.L., "Effects of contamination on Langmuir probe measurements in glow discharge plasmas", Journal Applied Physics. Vol. 41, No. 9, pp. 3428-32, July 1970.

32. Gagné, N., Fitchett, A. and Heckman, D., "X_s-band microwave interferometer for study of hypersonic turbulent wake on Range 5", DREV R-660/72, November 1972 (Unclassified).

33. Fitchett, A., "Resolution of the microwave lens system used in an X_s-band interferometer", DREV TN-1998/72, May 1972 (Unclassified).

34. Heald, M. and Wharton, C., "Plasma diagnostics with microwaves", John Wiley and Sons, 1965.

35. Sévigny, L., Heckman, D. and Emond, A., "Détermination du champ de vitesse du sillage d'une sphère hypersonique à l'aide de peignes de sondes ioniques", Canadian Journal of Physics, Vol. 50, No. 16, pp. 1842-55, August 1972.

36. Heckman, D., Sévigny, L., Fitchett, A., Emond, A. and Doyon, P. "Electron density behavior in the wake of 14,500 feet/second spheres", DREV R-680/72, December 1972. (Unclassified)

37. Sévigny, L. and Heckman, D., "Behavior of turbulent scales in hypersonic sphere wakes", DREV R-696/73, October 1973 (Unclassified).

38. Dionne, J.G.G., Heckman, D., Lahaye, C., Sévigny, L. and Tardif, L., "Fluid dynamic properties of turbulent wakes of hypersonic spheres", AGARD Conference Proceedings No. 93 of the Specialists' Meeting on Turbulent Shear Flow, London, England, 13-15 September 1971.

39. Sévigny, L., Tardif, L., Dionne, J.G.G., Heckman, D. and Lahaye, C., "Hypersonic wake studies", submitted for publication to the Canadian Aeronautics and Space Institute Journal.

40. Szuszczewicz, E.P., "Area influences and floating potentials in Langmuir probe measurements", Journal Applied Physics, Vol. 43, No. 3, pp. 874-80, March 1972.

41. Sévigny, L., "Exploration of space-time correlation functions", DREV TN 1844/69, October 1969 (Unclassified).

42. Favre, A.J., "Review on space-time correlations in turbulent fluids", Journal Applied Mechanics, Vol. 32, No. 6, pp. 241-257, June 1965.

43. Lane, F., "Comparison of measured space-time correlations of turbulent ion density fluctuations with predictions based on a mathematical model", General Applied Science Laboratories, Inc., Technical Report No. 668, September 1967 (Unclassified).

44. Lane, F., "Comparison of measured space-time correlations of turbulent ion density fluctuations with predictions based on an anisotropic mathematical model", General Applied Science Laboratories, Inc., Technical Report No. 689, March 1968 (Unclassified).

45. Shkarofsky, I.P., "Turbulence functions useful for probes (space-time correlation) and for scattering (wave-number frequency spectrum) analysis", Canadian Journal of Physics, Vol. 46, No. 23, pp. 2683-2702, December 1968.

DREV R-690/73 (UNCLASSIFIED)

CRDV, C.P. 880, Courcelette, Qué. - Conseil de recherches pour la défense

"Absolute Electron Density Measurements in Turbulent Hypersonic Sphere Wakes with Langmuir Probes" D. Heckman, L. Sévigny et A. Emond.

On a mesuré dans un des tunnels balistiques du Centre de recherches pour la défense, Valcartier (CRDV), la valeur absolue de la densité des électrons se trouvant dans le sillage ionisé produit par une sphère hypersonique de 2.7 pouces de diamètre, projetée à une vitesse de 14,500 pieds/seconde, dans de l'air à 10 torr. La technique expérimentale utilise des sondes de Langmuir dont les possibilités théoriques pour une telle expérience ont été démontrées par G.W. Sutton. Un soin tout particulier a été apporté à la réalisation de certains détails de l'expérience, telles la propreté des sondes, la minimisation des perturbations de l'écoulement et la réduction de l'intensité des ondes de choc réfléchies. La valeur de la densité électronique déduite des données fournies par les sondes de Langmuir est en accord avec celle obtenue par des mesures simultanées à l'aide d'un interféromètre micro-onde. On a également déterminé le comportement du potentiel de plasma dans le sillage. Celui-ci semble avoir tendance à se maintenir près du potentiel de la sonde la plus fortement polarisée, mais on n'a pu établir la raison de ce comportement. En conclusion, on suggère d'autres applications possible de l'appareillage expérimental. (N C)

DREV R-690/73 (UNCLASSIFIED)

CRDV, C.P. 880, Courcelette, Qué. - Conseil de recherches pour la défense

"Absolute Electron Density Measurements in Turbulent Hypersonic Sphere Wakes with Langmuir Probes" D. Heckman, L. Sévigny et A. Emond.

On a mesuré dans un des tunnels balistiques du Centre de recherches pour la défense, Valcartier (CRDV), la valeur absolue de la densité des électrons se trouvant dans le sillage ionisé produit par une sphère hypersonique de 2.7 pouces de diamètre, projetée à une vitesse de 14,500 pieds/seconde, dans de l'air à 10 torr. La technique expérimentale utilise des sondes de Langmuir dont les possibilités théoriques pour une telle expérience ont été démontrées par G.W. Sutton. Un soin tout particulier a été apporté à la réalisation de certains détails de l'expérience, telles la propreté des sondes, la minimisation des perturbations de l'écoulement et la réduction de l'intensité des ondes de choc réfléchies. La valeur de la densité électronique déduite des données fournies par les sondes de Langmuir est en accord avec celle obtenue par des mesures simultanées à l'aide d'un interféromètre micro-onde. On a également déterminé le comportement du potentiel de plasma dans le sillage. Celui-ci semble avoir tendance à se maintenir près du potentiel de la sonde la plus fortement polarisée, mais on n'a pu établir la raison de ce comportement. En conclusion, on suggère d'autres applications possible de l'appareillage expérimental. (N C)

DREV R-690/73 (UNCLASSIFIED)

CRDV, C.P. 880, Courcelette, Qué. - Conseil de recherches pour la défense

"Absolute Electron Density Measurements in Turbulent Hypersonic Sphere Wakes with Langmuir Probes" D. Heckman, L. Sévigny et A. Emond.

On a mesuré dans un des tunnels balistiques du Centre de recherches pour la défense, Valcartier (CRDV), la valeur absolue de la densité des électrons se trouvant dans le sillage ionisé produit par une sphère hypersonique de 2.7 pouces de diamètre, projetée à une vitesse de 14,500 pieds/seconde, dans de l'air à 10 torr. La technique expérimentale utilise des sondes de Langmuir dont les possibilités théoriques pour une telle expérience ont été démontrées par G.W. Sutton. Un soin tout particulier a été apporté à la réalisation de certains détails de l'expérience, telles la propreté des sondes, la minimisation des perturbations de l'écoulement et la réduction de l'intensité des ondes de choc réfléchies. La valeur de la densité électronique déduite des données fournies par les sondes de Langmuir est en accord avec celle obtenue par des mesures simultanées à l'aide d'un interféromètre micro-onde. On a également déterminé le comportement du potentiel de plasma dans le sillage. Celui-ci semble avoir tendance à se maintenir près du potentiel de la sonde la plus fortement polarisée, mais on n'a pu établir la raison de ce comportement. En conclusion, on suggère d'autres applications possible de l'appareillage expérimental. (N C)

DREV R-690/73 (UNCLASSIFIED)

CRDV, C.P. 880, Courcelette, Qué. - Conseil de recherches pour la défense

"Absolute Electron Density Measurements in Turbulent Hypersonic Sphere Wakes with Langmuir Probes" D. Heckman, L. Sévigny et A. Emond.

On a mesuré dans un des tunnels balistiques du Centre de recherches pour la défense, Valcartier (CRDV), la valeur absolue de la densité des électrons se trouvant dans le sillage ionisé produit par une sphère hypersonique de 2.7 pouces de diamètre, projetée à une vitesse de 14,500 pieds/seconde, dans de l'air à 10 torr. La technique expérimentale utilise des sondes de Langmuir dont les possibilités théoriques pour une telle expérience ont été démontrées par G.W. Sutton. Un soin tout particulier a été apporté à la réalisation de certains détails de l'expérience, telles la propreté des sondes, la minimisation des perturbations de l'écoulement et la réduction de l'intensité des ondes de choc réfléchies. La valeur de la densité électronique déduite des données fournies par les sondes de Langmuir est en accord avec celle obtenue par des mesures simultanées à l'aide d'un interféromètre micro-onde. On a également déterminé le comportement du potentiel de plasma dans le sillage. Celui-ci semble avoir tendance à se maintenir près du potentiel de la sonde la plus fortement polarisée, mais on n'a pu établir la raison de ce comportement. En conclusion, on suggère d'autres applications possible de l'appareillage expérimental. (N C)

DREV R-690/73 (UNCLASSIFIED)

DREV, P.O. Box 880, Courcelette, Qué. - Defence Research Board of Canada

"Absolute Electron Density Measurements in Turbulent Hypersonic Sphere Wakes with Langmuir Probes" D. Heckman, L. Sévigny, A. Emond.

Measurements were carried out in the ballistic range facilities at DREV of the absolute electron density levels in the wakes of 2.7 inch diameter spheres flow at 14,500 feet/second in air atmospheres at 10 torr. The experimental technique involved the use of Langmuir probes, following the theoretical demonstration of feasibility of such an experiment by G.W. Sutton. Considerable attention was paid to details of the experiment, such as probe cleanliness, minimum flow disturbance and the minimization of reflected shocks. Electron density level estimates obtained with the Langmuir probes were in good agreement with electron density estimates derived from simultaneous measurements with a microwave interferometer. The behavior of the plasma potential in the wake was also determined; the plasma potential apparently attempted to maintain itself close to the potential of the most highly biased probes, but the reason for this behavior has not been established. This Report concludes with suggestions for further utilization of the equipment. (U)

DREV R-690/73 (UNCLASSIFIED)

DREV, P.O. Box 880, Courcelette, Qué. - Defence Research Board of Canada

"Absolute Electron Density Measurements in Turbulent Hypersonic Sphere Wakes with Langmuir Probes" D. Heckman, L. Sévigny, A. Emond.

Measurements were carried out in the ballistic range facilities at DREV of the absolute electron density levels in the wakes of 2.7 inch diameter spheres flow at 14,500 feet/second in air atmospheres at 10 torr. The experimental technique involved the use of Langmuir probes, following the theoretical demonstration of feasibility of such an experiment by G.W. Sutton. Considerable attention was paid to details of the experiment, such as probe cleanliness, minimum flow disturbance and the minimization of reflected shocks. Electron density level estimates obtained with the Langmuir probes were in good agreement with electron density estimates derived from simultaneous measurements with a microwave interferometer. The behavior of the plasma potential in the wake was also determined; the plasma potential apparently attempted to maintain itself close to the potential of the most highly biased probes, but the reason for this behavior has not been established. This Report concludes with suggestions for further utilization of the equipment. (U)

DREV R-690/73 (UNCLASSIFIED)

DREV, P.O. Box 880, Courcelette, Qué. - Defence Research Board of Canada

"Absolute Electron Density Measurements in Turbulent Hypersonic Sphere Wakes with Langmuir Probes" D. Heckman, L. Sévigny, A. Emond.

Measurements were carried out in the ballistic range facilities at DREV of the absolute electron density levels in the wakes of 2.7 inch diameter spheres flow at 14,500 feet/second in air atmospheres at 10 torr. The experimental technique involved the use of Langmuir probes, following the theoretical demonstration of feasibility of such an experiment by G.W. Sutton. Considerable attention was paid to details of the experiment, such as probe cleanliness, minimum flow disturbance and the minimization of reflected shocks. Electron density level estimates obtained with the Langmuir probes were in good agreement with electron density estimates derived from simultaneous measurements with a microwave interferometer. The behavior of the plasma potential in the wake was also determined; the plasma potential apparently attempted to maintain itself close to the potential of the most highly biased probes, but the reason for this behavior has not been established. This Report concludes with suggestions for further utilization of the equipment. (U)

DREV R-690/73 (UNCLASSIFIED)

DREV, P.O. Box 880, Courcelette, Qué. - Defence Research Board of Canada

"Absolute Electron Density Measurements in Turbulent Hypersonic Sphere Wakes with Langmuir Probes" D. Heckman, L. Sévigny, A. Emond.

Measurements were carried out in the ballistic range facilities at DREV of the absolute electron density levels in the wakes of 2.7 inch diameter spheres flow at 14,500 feet/second in air atmospheres at 10 torr. The experimental technique involved the use of Langmuir probes, following the theoretical demonstration of feasibility of such an experiment by G.W. Sutton. Considerable attention was paid to details of the experiment, such as probe cleanliness, minimum flow disturbance and the minimization of reflected shocks. Electron density level estimates obtained with the Langmuir probes were in good agreement with electron density estimates derived from simultaneous measurements with a microwave interferometer. The behavior of the plasma potential in the wake was also determined; the plasma potential apparently attempted to maintain itself close to the potential of the most highly biased probes, but the reason for this behavior has not been established. This Report concludes with suggestions for further utilization of the equipment. (U)